

NUCLEAR MOMENTS

NUCLEAR MOMENTS
OF
 ^{140}La , ^{147}Nd AND ^{149}Nd

by

ANTON ROBERT PIERCE, A.B., M.Sc.

A Thesis

Submitted to the Faculty of Graduate Studies

in Partial Fulfilment of the Requirements

for the Degree

Doctor of Philosophy

McMaster University

May 1970

DOCTOR OF PHILOSOPHY
(Physics)

McMASTER UNIVERSITY
Hamilton, Ontario.

TITLE: Nuclear Moments of ^{140}La , ^{147}Nd , and
 ^{149}Nd

AUTHOR: Anton Robert Pierce, A.B. (Rutgers),
M.Sc. (McMaster)

SUPERVISOR: Dr. R. G. Summers-Gill

NUMBER OF PAGES: ix, 128

SCOPE AND CONTENTS:

Using atomic beam magnetic resonance techniques the hyperfine structure (hfs) constants for the magnetic dipole and electric quadrupole interaction, A_J and B_J , have been measured for the following isotopes: 40-hour ^{140}La , 1.8-hour ^{149}Nd and 11-day ^{147}Nd .

For ^{140}La the hfs constants are (relative to the $J = 5/2$ state of 2D) $|A_{5/2}| = 55.9(4)$ MHz, $|B_{5/2}| = 38(4)$ MHz, $B_{5/2}/A_{5/2} > 0$. Application of the Fermi-Segrè relations in comparison with ^{139}La yields the nuclear moments; $\mu_I = (+)0.73(3)$ n.m., and $Q = (+)0.11(4)$ b. The adopted signs are based on Blok's measured sign of Q for ^{140}La .

For ^{149}Nd the hfs constants are: $|A_4| = 91.0(19)$ MHz, $|B_4| = 266(53)$ MHz, and $B_4/A_4 > 0$. Comparison with ^{145}Nd yields $\mu_I = (-)0.350(10)$ nm., and $Q = +1.3(3)$ b. The signs of these moments are based on $Q > 0$ as indicated by nuclear systematics in this region.

For ^{147}Nd the hfs constants are $|A_4| = 143(4)$ MHz, $|B_4| = 181(64)$ MHz, and $B_4/A_4 > 0$. Comparison with ^{145}Nd yields $|\mu_I| = 0.553(15)$ n.m., $|Q| = 0.9(3)$ b and $\mu_I/Q < 0$.

The error in the ^{140}La magnetic moment allows for a possible 2% hfs anomaly. The quadrupole moments allow for a possible 25% error in the core polarization correction (Sternheimer).

These results are discussed in terms of the shell model, the quasi-particle model, and the Nilsson model.

ACKNOWLEDGEMENTS

It is a privilege to thank all those who have helped make this work possible. Special thanks must go to the following:

Professor R. G. Summers-Gill for his unfailing interest and patience, and for many stimulating speculations.

Professors M. W. Johns and W. W. Smeltzer, who were members of my Supervisory Committee, for their guidance.

Drs. J. A. Cameron and C. V. Stager for many useful discussions.

Drs. R. A. Deegan and J. C. Waddington for their encouragement when it was needed most.

Dr. G. M. Stinson for his kindness during the early days of learning to drive the machine.

Mr. J. Z. Melkvi for the academic folk dancing lessons.

Mr. R. G. H. Robertson for his unfailing assistance kindly given in performing these experiments. S. G. Hussein, who rendered valuable assistance during the runs.

Finally to Mr. D. A. Dohan, Mr. R. A. McPhail and Mr. D. B. Kenyon for their many pleasantries.

The Health Physics Group, Dr. J. A. Harvey and Messrs. D. Whiteford and A. Roncari for advice and help in mopping up.

The reactor staff kindly provided about 100,000,000,000,000,000,000 neutrons for these experiments.

Mrs. H. Kennelly performed miracles in typing this work from an incredibly marked up and hashed over scroll of hieroglyphics.

My mother for her faith and my wife, Heather, for her love.

This work was supported by grants in aid to the group from the National Research Council of Canada. Stipends to the author from the Ontario Graduate Fellowship Programme are very gratefully acknowledged. Aid was provided by the Libraries and Information Systems Centre of Bell Telephone Laboratories, Inc. in the preparation of the drawings.

TABLE OF CONTENTS

CHAPTER		<u>Page</u>
I	INTRODUCTION	1
II	NUCLEAR MOMENTS AND MODELS	5
	A. Multipole Moment Operators	7
	B. Shell Model	11
	C. Configuration Mixing	19
	D. Nilsson Model	25
III	HYPERFINE STRUCTURE	31
	A. Atomic Hamiltonian	33
	B. Magnetic Dipole Interaction	35
	C. Electric Quadrupole and Higher Order Interactions	39
	D. Hyperfine Structure Anomaly	43
	E. Sternheimer Correction	47
	F. Zeeman Effect	50
	G. Induced Magnetic Dipole Transitions	55
IV	THEORY OF EXPERIMENT AND RESULTS	61
	A. Operation of the Apparatus	61
	B. Computer Programmes	69
	C. General Experimental Considerations	72
	D. The ¹⁴⁰ La Experiments	79
	E. The ¹⁴⁹ Nd Experiments	91
	F. The ¹⁴⁷ Nd Experiments	98

CHAPTER		<u>Page</u>
V	DISCUSSION	103
	A. The ^{140}La Results	103
	B. The ^{149}Nd Results	109
	C. The ^{147}Nd Results	115
	D. Summary	118
	BIBLIOGRAPHY	120

LIST OF FIGURES

<u>Figure</u>		<u>Page</u>
3.1	Zeeman Splitting in a Magnetic Field	53
4.1	Principles of Operation of Apparatus	62
4.2	Exit Beam Profile	64
4.3	Background Interpolation and Resonance Line Shape	82
4.4	The ^{140}La Resonances	85
4.5	χ^2 as function of $A_{5/2}$ and $B_{5/2}$ for ^{140}La	87
4.6	The ^{149}Nd resonances	95
4.7	The ^{147}Nd Resonances	100
5.1	The Nuclear Moments of ^{149}Nd and the $I = 5/2$ Nilsson states.	112
5.2	Ground State Quadrupole Moments of odd-A Neodymium Isotopes.	116

LIST OF TABLES

TABLE		<u>Page</u>
4.1	Electronic Equipment	68
4.2	The ^{140}La Resonances	89
4.3	The ^{149}Nd Resonances	96
4.4	The ^{147}Nd Resonances	101
5.1	Possible β^- transitions for $^{149}\text{Pr} \rightarrow ^{149}\text{Nd}$ on Nilsson Model	114

CHAPTER I
INTRODUCTION

Any observable quantity q of a physical system can be expressed as the expectation value of an operator O with the system's wave function:

$$q = \langle \psi | O | \psi \rangle.$$

Since the nuclear multipole operators can be developed quite rigorously from electromagnetic theory, so far as the calculation of nuclear moments is concerned, nuclear theory is the problem of developing the nuclear wave function, $|\alpha I m\rangle$ (where I = total angular momentum, M is its magnetic projection and α stands for all other quantum numbers which may be required to specify the state). At first sight the nuclear wave function should be an impossibly complicated creature which must faithfully describe the space, spin, and isospin co-ordinates of each of the A nucleons. To reduce the number of co-ordinates, and thereby make the nuclear problem tractable, various nuclear models have been proposed. Of course the success of any model must be gauged by its agreement with experiment. Proceeding by this comparison using several nuclear models one is able to pick out the important physical content of the true nuclear wave function as it is represen-

ted by the models.

The model wave function $|\phi\rangle$ is the solution of the Schrödinger equation $H_{\text{mod}} |\phi\rangle = E|\phi\rangle$, and unless H_{mod} (model Hamiltonian) is equal to the true Hamiltonian discrepancies will result (as is always the case). These discrepancies can be viewed as the inability of the model potential to satisfactorily account for the effects of the true inter-nucleon potential. The left-over bit is known as the residual interaction. The effect of the residual interaction is to mix various model states so that in the presence of the residual interaction,

$$|\phi\rangle + \alpha|\phi\rangle + \beta|\phi_1\rangle + \gamma|\phi_2\rangle + \dots$$

where the ϕ_n are eigenfunctions of H_{mod} . Provided that $\alpha \gg \beta, \gamma \dots$ perturbation theory can be used and the wave function can be calculated, in principle, to any desired degree of accuracy. This approach has been very successful in atomic spectroscopy where the residual interaction due to electron-electron repulsion, spin-orbit coupling, and other higher order effects such as the spin-spin coupling are small compared to the central Coulomb potential which appears in the electronic model Hamiltonian.

However, in the nuclear case, residual interaction is of the same order of magnitude as the model potential and a great deal of interconfiguration mixing can be expected.

As will be shown later, magnetic moments are sensitive to interconfiguration mixing and this fact makes them useful tests of the models. For example, it was used here to determine the composition of the ^{140}La ground state.

Nuclear quadrupole moments are particularly sensitive to the degree of nuclear deformation and so they can also act as a kind of nuclear model selector. The ^{149}Nd results led to interpretation of that nucleus in terms of the Nilsson model.

In the work reported here, the simple attempts at fitting models and configurations to measured nuclear moments are of really secondary import to the experimental values themselves, which should be viewed as fundamental nuclear constants entering on an equal footing with spin, binding energy, or half life. That is, the nuclear moments must be reproduced by any future calculation which hopes to fully explain nuclear structure.

Atomic beam magnetic resonance (ABMR) represents an extremely important technique for measuring nuclear moments. For radioactive isotopes, that method often provides the only way that the moments of certain nuclei can be measured. Certainly, such was the case for one of the isotopes reported here - 1.8 hr. ^{149}Nd .

a) The half life is too short to permit growth of a host crystal for nuclear magnetic resonance or

electron paramagnetic resonance studies.

- b) The number of radioactive atoms that can be produced in a sample is too small to permit observation of the hyperfine structure by optical spectroscopy.

In Chapter II of this work the theory of the multipole operators and the values based on several different nuclear models are presented. Chapter III deals with the atomic hfs interaction and the requisite corrections to nuclear moments determined from hyperfine structure constants. The theory and operation of the apparatus and the experimental results are given in Chapter IV. Chapter V concerns itself with a discussion of those results.

CHAPTER II

NUCLEAR MOMENTS AND MODELS

Although the actual form of the nuclear force has not been established to anything like the certitude of the Coulomb force and the much smaller magnetic forces that determine atomic structure, several of its features can be made out. Mass spectroscopic studies reveal that, on the average, the binding energy per nucleon is nearly constant at about 8 MeV per nucleon. The relative constancy of the specific binding energy indicates that the nuclear force becomes saturated. Saturation implies both that the attractive nuclear force has a very short range and that it becomes repulsive for even smaller values of inter-nucleon separation. The repulsive core is required to keep nuclei from collapsing and, indeed, to ensure that the specific binding energy doesn't increase with increasing A . The core repulsion and the longer-range attractive potential can be pictured as compensating each other to yield an overall attractive effective potential. Then, provided one doesn't look too closely at details, the nucleus itself becomes a localized region of attractive potential energy. That is, a gross nuclear potential is envisaged, built up as an average of all the effective

internuclear potentials. In addition to saturation, the nuclear force also exhibits the pairing property. That is the nucleons tend to couple pair-wise to spin zero. One manifestation of the pairing force is the fact that all known even-even nuclei have zero spin ground states.

Generally the starting point of a nuclear model is the assumption of some specific form for this nuclear potential. Of course, to be useful, the chosen potential must be readily soluble, either analytically or by computer, when it is substituted into the Schrödinger equation. The justification for generating this average nuclear potential is based on the Hartree-Fock approach to the concept of a self-consistent field. Implicit is the assumption that the nucleons move independently of one another.

This independence means that it should be possible to describe at least some nuclear properties by a single particle model in which the A^{th} nucleon is assumed to move in the model potential contributed by the other $A-1$ nucleons. For example, once the model potential has been chosen and the Schrödinger equation is solved it is possible to obtain the model's prediction for the nuclear moments.

A. Multiple Moment Operators

The electro-magnetic properties of the atomic nucleus are due to the charge and current distributions of the constituent nucleons. The static electromagnetic fields set up by an arbitrary charge-current system can be written in terms of the electric scalar potential V and the magnetic vector potential \vec{A} . Classically, at a point \vec{r} from some origin these potentials are:

$$V(\vec{r}) = \int \frac{\rho(\vec{r}')}{|\vec{r}-\vec{r}'|} d^3\vec{r}' \quad A(\vec{r}) = \int \frac{\vec{j}(\vec{r}')}{|\vec{r}-\vec{r}'|} d^3\vec{r}' \quad (2.1)$$

where $\rho(\vec{r}')$ is the electric charge at a source point \vec{r}' and $\vec{j}(\vec{r}')$ is the current density due to the motion of the charges. At points outside the charge-current system V and \vec{A} are given by [Schw-55]

$$V = \sum_{k=0}^{\infty} \sum_{\mu=-k}^k \frac{C_k^{(\mu)}(\theta, \phi)}{r^{k+1}} \cdot E_k^{\mu}$$

$$\vec{A} = \sum_{k=1}^{\infty} \sum_{\mu=-k}^k \frac{i}{r^{k+1}} (-i\vec{r} \nabla \times C_k^{(\mu)}(\theta, \phi)) \cdot M_k^{\mu}$$

Here $C_k^{(\mu)}(\theta, \phi) = \sqrt{\frac{4\pi}{2k+1}} Y_k^{\mu}(\theta, \phi)$ where $Y_k^{\mu}(\theta, \phi)$ is the normalized spherical harmonic of order k, μ and E_k^{μ} and M_k^{μ} are the electric and magnetic multipole moments, respectively.

The utility of such expressions arises because usually the series expansion in E_k and M_k converges very quickly. Thus, the fields can be well described by only considering the lowest order multipole. When the system is the atomic nucleus, expression of the nuclear electromagnetic properties in terms of the multipoles is most useful because these multipoles are intrinsic nuclear quantities and can't depend on the position of the field point.

Under the assumption that we only attempt to measure the multipole moments using fields external to the nucleus, the nuclear moments M_k^μ and E_k^μ can be found from equation 2.1 [Schw-55]. The nuclear charge is due to the Z protons; thus the electric multipole operator is

$$E_k^\mu = e \sum_{i=1}^Z r_i^k Y_k^\mu(\theta_i, \phi_i). \quad (2.2)$$

The nucleons have associated with their intrinsic spin of one half unit of angular momentum an intrinsic magnetization. For the free proton and free neutron this magnetization is expressible as a point magnetic dipole moment. Thus there are two contributions to the effective current density $\vec{j}(\vec{r})$ and these are written in terms of orbital and intrinsic spin g -factors, g_l and g_s for the neutrons and the protons. Then one can write

$$M_k^\mu = \mu_N \sum_{i=1}^A \nabla_i (r_i^k Y_k^\mu(\theta_i, \phi_i)) \cdot (g_\ell^{(i)} \frac{2 \vec{\ell}_i}{k+1} + g_s^{(i)} \vec{s}_i) \quad (2.3)$$

where $\mu_N = \frac{e\hbar}{2M_p c}$ is the nuclear magneton, and $g_\ell = 1$ for protons and $g_\ell = 0$ for neutrons. The intrinsic spin g -factors are +5.59 and -3.83 for protons and neutrons, respectively. These intrinsic spin g -factors can be pictured as being due to "orbital" motion of the nucleon's constituent π -mesons.

In a quantum-mechanical context, the static nuclear moments become the expectation values $\langle II | O_k^0 | II \rangle$, where the nuclear angular momentum is I and $|II\rangle$ denotes the nuclear state with magnetic quantum number equal to I . The operators O_k^0 are the appropriate multipole expressions in (2.2) or (2.3). Their parities are determined by noting that $\pi(\nabla r^k Y_k^\mu) = (-1)^{k+1}$, and $\pi(Y_k^\mu) = (-1)^k$. Thus

$$\begin{aligned} \pi(M_k^\mu) &= (-1)^{k+1} \\ \pi(E_k^\mu) &= (-1)^k. \end{aligned} \quad (2.4)$$

For states of definite parity, such as the nuclear states $|IM\rangle$, the expectation values of odd operators are zero. Referring to equation (2.4), this rule means that only even electric moments and odd magnetic moments can be non-zero. This result is in contrast to the classical case where no such restrictions apply for charge and current systems of arbitrary shape.

Another restriction also exists. Making use of

the Wigner-Eckhart theorem the nuclear moments are given by

$$\langle II | O_k^0 | II \rangle = \begin{pmatrix} I & k & I \\ -I & 0 & I \end{pmatrix} \langle I || O_k || I \rangle \quad (2.5)$$

where the double-barred symbol is a reduced matrix element and $O_k = E_k$ for k even, $O_k = M_k$ for k odd. The 3-j symbol vanishes unless the triad (I, I, k) can form a triangle.

Hence, only for $I \geq \frac{1}{2}$ can the nucleus have a non-zero magnetic moment. Similarly, unless $I \geq 1$, the quadrupole moment is zero.

B. Shell Model

The shell model of Mayer and Haxel, Jensen and Suess [Mayr-49, Haxl-49, Mayr-55] derives its name from its treatment of the motion of the nucleons in terms of orbits that have been primarily defined by a central potential. Thus, in analogy with the shells formed by the atomic electrons, nuclear shells arise by virtue of the model potential. In addition, a pairing force is invoked as a coupling rule that permits tremendous simplification of the problem.

The first step is to write down a potential that will roughly reproduce the attractive nuclear field. For that purpose a spherically symmetric oscillator well is chosen

$$V(r) \sim V_0 + \frac{1}{2} m\omega^2 r^2 \quad (V_0 < 0)$$

where m is the reduced mass of the system consisting of the single particle, mass M , and the rest of the nucleons, mass M_T , which generates the potential in which the particle moves. Solution of the Schrödinger equation for the harmonic oscillator potential yields a spectrum $E_N = \hbar\omega \left(\frac{3}{2} + N\right) + V_0$ where N is a positive integer. Each harmonic oscillator level of energy E_N is composed of $(N+1)(N+2)$ degenerate states which can be chosen to have definite orbital angular momentum, viz. $|N \ell m_\ell m_s\rangle$. In order to remove this degeneracy and, indeed, to more realistically reproduce observed nuclear

properties, two additional terms are added to the parabolic well so that

$$V = V_0 + \frac{1}{2} m\omega^2 r^2 + C \vec{l}^2 + D\xi(r) \vec{l} \cdot \vec{s}. \quad (2.6)$$

The term in \vec{l}^2 splits the levels E_N into states whose energies depend on l also. The spin-orbit term further splits each of these levels into two characterized by $j = l + \frac{1}{2}$ and $j = l - \frac{1}{2}$. The eigenfunctions are then written as $|n l j m_j\rangle$ where the change to n signifies a redefinition of the radial quantum number and m_j is the z-axis projection of \vec{j} . The relative strengths of ω , C , and D are adjusted to produce gaps in the spectrum at the experimentally observed magic numbers.

The building up of the various nuclear species is similar to what happens in the chemical periodic table. Only $2j+1$ nucleons can be accommodated in each level $(n l j)$. Because of charge independence, the model predicts that protons and neutrons should have the same states available to them. However, for $Z > 50$, Coulomb repulsion becomes so important that a re-ordering of the proton levels takes place. The Coulomb repulsion is also responsible for the neutron excess in stable nuclei which means that, for $A > 60$, the neutrons and protons are filling different shell model states. In the extreme single particle shell model, the ground state nuclear spin for odd A nuclei is determined by the

j -value of the last unpaired nucleon. While this is generally observed to be true there are some notable exceptions. For odd-odd nuclei, the shell model proper can only predict $\vec{I} = \vec{j}_p + \vec{j}_n$ where \vec{j}_p and \vec{j}_n are the j -values of the odd proton and odd neutron respectively. The different possible values of nuclear spin would be degenerate.

Clearly some residual force must be introduced, that is, a force acting between the odd proton and odd neutron or, more generally, between all the nucleons in unfilled shells. The residual interaction does not necessarily resemble the "real" internucleon potential but, rather, seeks to reproduce that part of the real internucleon potential that has not been included in the central shell-model potential. Nordheim, and later Brennen and Bernstein, [Nord-51, Bren-60] have been able to enunciate rules which correctly predict the ground state spin in an impressively large number of cases. These authors assume that the residual interaction can be written as a contact or delta-function potential.

The shell model magnetic dipole moment μ_I is found using equation (2.3)

$$\mu_I = \left\langle I, m=I \left| \mu_N \sum_{i=1}^A \nabla_i (r_i Y_{10}^0) (g_l^{(i)} \vec{l}_i + g_s^{(i)} \vec{s}_i) \right| I, m=I \right\rangle .$$

Operating with ∇_i on $r_i Y_{10}^0$ yields the unit vector \hat{z}_i which, when multiplied by the term involving the g -factor, means

that only the Z components of \vec{l}_i and \vec{s}_i need be considered.

The extreme single particle model attributes the nuclear spin to the last unpaired nucleon so that, for this model, the sum over the A nucleons is dropped and the equation becomes

$$\mu_I = \mu_N \langle II | g_\ell l_z + g_s s_z | II \rangle. \quad (2.7)$$

The generalized Landé formula for any vector operator \vec{O} gives

$$\langle IM | \vec{O} | IM \rangle = \frac{\langle IM | \vec{I} | IM \rangle \langle IM | \vec{I} \cdot \vec{O} | IM \rangle}{I(I+1)}. \quad (2.8)$$

In the shell model the state $|IM\rangle$ is identical to $|n\ell j\rangle$.

Hence

$$\begin{aligned} \mu_I &= \mu_N \frac{\langle II | I_z | II \rangle \langle II | g_\ell \vec{I} \cdot \vec{l} + g_s \vec{I} \cdot \vec{s} | II \rangle}{I(I+1)} \\ &= \frac{\mu_N}{I+1} (g_\ell \langle \vec{I} \cdot \vec{l} \rangle + g_s \langle \vec{I} \cdot \vec{s} \rangle). \end{aligned} \quad (2.9)$$

The dot products are evaluated using $\vec{l}^2 = (\vec{I} - \vec{s})^2 = \vec{I}^2 + \vec{s}^2 - 2\vec{I} \cdot \vec{s}$, etc. The single particle moment is

$$\mu_I = \frac{I}{2} ((g_\ell + g_s) + (g_\ell - g_s) \times \frac{\ell(\ell+1) - s(s+1)}{I(I+1)}) \mu_N. \quad (2.10)$$

If it is assumed that the nucleons retain their free particle g-values in the nucleus then moments predicted by (2.10) are known as the Schmidt values. Obviously, the

value of the moment depends on which shell model state $|n\ell j\rangle$ is involved. As such, measurement of μ should help to determine the correct character, in particular the ℓ value, of any given nuclear state.

For odd-odd nuclei the simplest nuclear wave function is

$$\sum_{m_n, m_p} \langle j_p m_p j_n m_n | j_p j_n IM \rangle |j m_p\rangle |j m_n\rangle$$

where the kets $|j m_p\rangle$, $|j m_n\rangle$ stand for the states $|n\ell j\rangle$ of the last odd proton and the last odd neutron, respectively. Application of j-j coupling yields the odd-odd Schmidt value

$$\mu_{o-o} = \frac{I}{2} [(g_p + g_n) + (g_p - g_n) \frac{j_p(j_p+1) - j_n(j_n+1)}{I(I+1)}] \quad (2.11)$$

where g_p and g_n are the g-factors based on the Schmidt values for the odd proton and neutron, i.e. $g_p = \frac{(\mu) \text{ Schmidt}}{j_p \mu_N}$, etc. Alternatively, the proton and neutron g-factors can be taken from the measured magnetic moments of neighbouring odd-A nuclei. If the latter procedure is adopted quite good agreement with experiment usually results. The reason for the improvement is that the empirical g-factors allow for interconfiguration mixing in the neutron and proton single particle wave functions.

The nuclear quadrupole moment is defined to be $\frac{2}{e} \sqrt{\frac{4\pi}{5}}$ times the $\mu=0$ component of E_2^μ , the factor of two being due to historical development. Thus $Q = 2 \left\langle \sum_{i=1}^Z r_i^2 Y_2^0(\theta_i \phi_i) \right\rangle$ since the neutrons are uncharged. If it is assumed that there

is only one proton in the orbit $|nlj\rangle$, the quadrupole moment for the single particle is

$$Q_{sp} = 2 \langle nlj | r^2 Y_2^0 | nlj \rangle.$$

The sum over Z has been reduced to the one unpaired proton since the core, on the basis of the shell model, represents a spherical charge distribution which cannot possess a quadrupole moment itself*. Evaluation of the matrix element yields:

$$Q_{sp} = - \frac{2j-1}{2j+2} \langle nl | r^2 | nl \rangle \leq 0. \quad (2.12)$$

Without any specific reference to the shell model, electron scattering data reveals that the nuclear r.m.s. radius is $1.2 A^{1/3} \times 10^{-13}$ cm. Hence $Q_{s.p.} \sim -A^{2/3} \times 10^{-26}$ cm². With $A \approx 150$, then, $Q_{s.p.} \sim -.25b$ for odd-proton nuclei.

For an odd-neutron nucleus the single particle model seemingly predicts zero quadrupole moment. However the motion of the odd neutron causes a "wobble" of the remaining core particles so as to keep the centre of mass fixed. On the average the odd neutron sees the rest of the nucleus as a blob of charge Ze , a distance r_n/A away. Hence the quadrupole moment operator $r^2 \rightarrow Z \left(\frac{r_n}{A}\right)^2$, or $Q_n \approx \frac{Z}{A^2} Q_{s.p.} \approx \frac{1}{375} Q_{sp}$ (odd proton) for $A \approx 150$.

* See below in Section D.

A more realistic approach is taken if only those particles in closed shells are treated as forming an inert core. In general, there may be k active particles in the $|n\ell j\rangle$ orbit where k is odd. For $k \geq 3$, the matrix elements of the magnetic dipole and electric quadrupole operators can be reduced, using coefficients of fractional parentage (cfp), to the matrix elements for $k-2$ particles. The process can be continued until the matrix element for k particles, $\langle j^k | O | j^k \rangle$, is reduced to a single particle matrix element. Each shell can accommodate $2j+1$ particles and whenever $k > j + \frac{1}{2}$, it is more convenient to speak of K holes where $K = 2j+1-k$. Hole states can be generated from particle states by reversing the signs of the m_j . Thus, the matrix elements for k particles and K holes are related by a phase factor

$$\langle (n\ell j)^k_I | O_\lambda | (n\ell j)^k_I \rangle = (-1)^{\lambda+1} \langle (n\ell j)^K_I | O_\lambda | (n\ell j)^K_I \rangle.$$

For magnetic moments $\lambda=1$, so that the phase factor is positive, while for quadrupole moments $\lambda=2$ and the phase factor is negative. This means that $\mu((j)^K) = \mu((j)^k)$, and $Q((j)^K) = -Q((j)^k)$.

Even more informative relationships can be derived.

For the magnetic moment, the trick is to note that, in

$$g_I = \frac{|\Sigma \vec{\mu}_i|}{|\Sigma \vec{j}_i| \mu_N},$$

both $\Sigma \vec{j}_i$ and $\Sigma \vec{\mu}_i$ are vector operators, that

is, $\lambda=1$. Thus, their expectation values in the state $|(n\lambda j)^k, II\rangle$ both have the same cfp in the reduction to single particle matrix elements. Hence the form is

$$(g_I)_k = \frac{\mu}{j} \times \frac{\text{cfp}}{\text{cfp}} = (g_I)_{s,p},'$$

and the nuclear g-factor cannot depend on the number of particles in the orbital. If nuclear g-factors are observed to change as an orbit is apparently filled, (e.g. the neodymium isotopes), then the source lies elsewhere - such as in configuration mixing.

For the electric quadrupole moment, no such cancellation involving the ratio of identical cfp's occurs, and so Q is dependent on the number of particles in a given orbit. For states of the type $|(n\lambda j)^k; I=j, I\rangle$,

$$Q = \frac{2J - 2k + 1}{2j - 1} Q_{s.p.} \quad (2.13)$$

where $Q_{s.p.}$ is the single particle moment given by eq. 2.12.

We note that as k increases the magnitude of Q decreases until, at one nucleon more than a half-filled orbit, the sign of Q reverses. For states of the type $|(n\lambda j)^k, I=j-1, I\rangle$, the relationship is changed; thus, for $(2f_{7/2})^3_{I=5/2}$,

$$Q \approx 3(Q_{2f_{7/2}})_{s.p.} \quad [\text{Mayr-55}].$$

C. Configuration Mixing

It is an experimental fact that most nuclear magnetic moments deviate considerably from the single particle Schmidt values. Furthermore, quadrupole moments, notably in the regions corresponding to $A \sim 150-170$ and $A \sim 240$, are 10-30 times larger than the shell model predictions. This latter effect is due to permanent deformation of the nucleus, and the moments of deformed nuclei will be discussed in the section on the Nilsson model.

In deriving the Schmidt values it was assumed that the nucleons retained their free-particle g -values inside the nucleus. The nucleons owe their charge and current densities to their constituent mesons. Very roughly, the proton can be viewed as a "bare" nucleon which is coupled virtually to a positive π meson. Similar considerations hold for the neutron. In the nucleus, the nucleons can fairly readily exchange these mesons, thereby setting up currents which may be expected to alter the free g -values. These exchange effects have been deduced from measurements on some light mirror-nucleus pairs and are found to be only $\sim .1$ to $.2$ n.m. [See, for example, Habe-64]. Because departures from the Schmidt values are usually 0.5 to 1 n.m., meson exchange can not be solely responsible for them.

Any possible velocity dependence on the inter-nucleon force, that is velocity dependence of the appropriate

residual interaction, can also alter the free-nucleon g -values. This comes about because the momentum \vec{p} becomes $\vec{p} - \frac{e}{c} \vec{A}$ for systems in the presence of an electromagnetic field. If the residual potential v_{ij} is velocity dependent so that $v_{ij} = v_{ij}(0) + v_{ij}(\vec{p})$, then an additional term must be included in the orbital g -factor. There is still no clear-cut answer regarding just what the velocity dependence of the nuclear potential is but it is unlikely the dependence would change rapidly with A . Thus, quite different moments in neighbouring nuclei can be taken to be an indication of configuration differences.

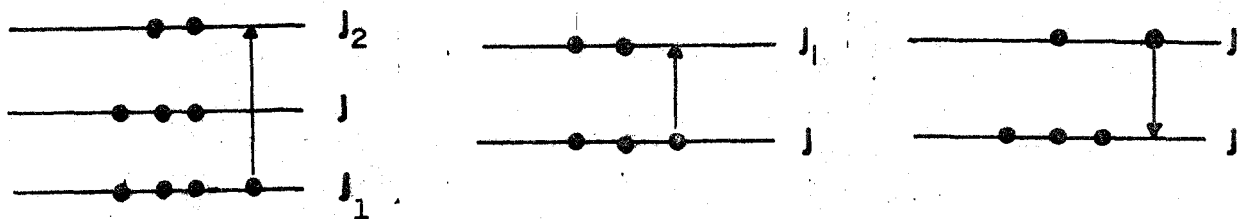
The most successful way of describing departures from the Schmidt limits is through interconfiguration mixing of model states [Blin-54, Arma-55, Noya-58]. Presuming that the nuclear wave function can be written as $|IM\rangle = \phi_0 + \sum_n \alpha_n \phi_n$, where ϕ_0 represents the model state (e.g. the shell model state $(n\ell j)^k$ which best approximates the true nuclear wave function, then

$$\langle II | \vec{\mu} | II \rangle = \langle \phi_0 | \vec{\mu} | \phi_0 \rangle + 2 \sum_n \alpha_n \langle \phi_0 | \vec{\mu} | \phi_n \rangle + \dots$$

Since the magnetic moment operator can connect states $|n\ell j \pm \frac{1}{2}\rangle$ sizable correction to the Schmidt values $\langle \phi_0 | \vec{\mu} | \phi_0 \rangle$ can thus result in first order. The shell model wave function should be a good description for nuclei which are doubly magic ± 1 nucleon and indeed it is observed these nuclei have moments

which are close to the Schmidt values. However ${}^{209}_{83}\text{Bi}_{126}$ has a moment which is only half its Schmidt value. Part of the reason for this is due to the fact that ${}^{208}_{82}\text{Pb}_{126}$ is doubly magic only in pure j - j coupling.

Noya et al (op cit) consider the several possible cases. For example, suppose that orbits j_1 and j_2 contain even numbers of nucleons paired off to zero angular momentum and orbit j has an odd number of nucleons. Then, if a nucleon jumps from orbit j_1 to j_2 through its interaction with the nucleons in orbit j we will have three active orbits j , j_1 and j_2 all contributing to μ . Other processes are also possible, such as a nucleon leaving orbit j to go into j_i , or, conversely, a particle being excited into j from j_i



with similar terms for the other processes.

Assuming that the residual interaction can be written as a δ -function force, Noya et al. show that the corrections to μ , denoted by $\delta\mu$, from these three types of excitations

have a common factor

$$\delta\mu \sim - [1 + (-1)^{\ell+1/2-j} (j+\frac{1}{2})] (g_s - g_\ell). \quad (2.14)$$

Examination of the measured moments for odd-neutron nuclei reveals that the vast majority lie within, rather than on, the Schmidt values. These are just the corrections predicted by (2.14). Similar considerations hold for odd-proton nuclei. In the special case of $p_{1/2}$ nuclei, the correction vanishes - indeed it is observed that the moments of these nuclei usually do lie close to their Schmidt values. Furthermore the deviations $\delta\mu$ for mirror nuclei show

$$\frac{(\delta\mu)_{\text{odd } Z}}{(\delta\mu)_{\text{odd } N}} \approx -1.2 = \frac{(g_s - g_\ell)_p}{(g_s - g_\ell)_n}$$

which again confirms (2.14).

Quite good quantitative agreement results when the authors consider specific cases. Encouragingly, the results are fairly insensitive to the depth and shape of the shell model potential used. This insensitivity implies that if the members of an odd isotope or isotone group show different departures from their Schmidt values, the cause is unusual interconfigurational effects and not minor changes in the nuclear potential.

For an odd-odd nucleus, Cain [Cain-56] has shown that if the departures of neighbouring odd-Z and odd-N nuclear moments from their Schmidt values are due to inter-

configuration mixing - so that

$$\mu_{\text{odd } N} = \langle \phi_0 | \mu | \phi_0 \rangle + 2 \sum_n \alpha_n \langle \phi_0 | \mu | \phi_n \rangle + \dots,$$

then the correction to the odd-odd moment is

$$\delta\mu = 2 \left(\sum_{\substack{\text{odd} \\ n}} \alpha_n \langle \phi_n^0 | \mu | \phi_n' \rangle + \sum_{\substack{\text{odd} \\ p}} \alpha_p \langle \phi_p^0 | \mu | \phi_p' \rangle \right). \quad (2.15)$$

But (2.15) is just the amount included when effective moments for the odd proton and odd neutron, as determined by the measured magnetic moments of neighbouring odd nuclei, are used.

Attention is now paid to a model or, perhaps more properly, a scheme of calculations which has the configuration mixing approach built in. The action of the nuclear force causes the mixing of several nuclear states. Thus any one particle really is distributed over several model states and, as such, it is known as a quasi-particle. Because some of these states may be quite high in energy relative to the ground state, it is also appropriate to include contributions (usually quite high in energy) due to vibrations of the nuclear core. In the calculation of Kisslinger and Sorenson [Kiss-63] the residual interaction is chosen to be the sum of a short range pairing term and a longer range quadrupole force based on the observation of vibrational spectra in even-even nuclei.

The contributions to the total Hamiltonian are split

into a pairing contribution - based on superconductivity theory [Bohr-59]-and the (quadrupole) phonon contribution. The development of the theory utilizes the notation of second quantization in which all nucleons in filled shells are treated as a vacuum state $|0\rangle_0$. The creation and annihilation operators A_j^+ and A_j are used to enumerate the contributions of the active orbitals.

In particular, the magnetic dipole and electric quadrupole operators can be separated in terms of quasi-particle and phonon contributions. The matrix elements for these operators have been worked out [Kiss-op cit] for several nuclei. In general, the resulting values for magnetic moments are inward from the Schmidt value as is to be expected because of the allowance for configuration mixing. Because the phonon amplitude represents a dynamic distortion, the results of Kisslinger and Sorenson do not predict quadrupole moments which are significantly larger than those of the shell model.

D. Nilsson Model

As experimental values for quadrupole moments became available it was apparent that there existed regions of A for which the nuclear quadrupole moments were several times larger than the values predicted by the shell model. In addition, these moments were, without exception, positive. Rainwater [Rain-50] concluded that the nucleus was shaped as a prolate ellipsoid and the large quadrupole moment was proportional to the degree of deformation. Consider a uniformly charged ellipsoid with charge density $\rho = \frac{Ze}{V} = \frac{3}{4} \frac{Ze}{\pi ab^2}$ where a and b are the lengths of the semi-major axes, respectively. If the symmetry axis is denoted by z' , then the quadrupole moment with respect to the z' axis is [Pres-62, Chapter 4]

$$\begin{aligned} Q' &= \frac{2}{e} \int \rho r^2 Y_2^0 dV \sim \frac{1}{e} \int \rho (3z'^2 - r^2) dV \\ &= \frac{2}{5} Z (a^2 - b^2) \sim Z R_0^2 \delta + O\left(\frac{2}{3} \delta^2\right) \end{aligned} \quad (2.16)$$

where δ is the deformation parameter $\delta = \frac{1}{2} \frac{a^2 - b^2}{a^2}$, and R_0 is the equivalent spherical radius defined by $R_0^3 = ab^2$.

Hence the intrinsic quadrupole moment Q' is approximately $Z\delta$ times larger than the single particle moment. This possibility is excluded in the shell model because of the inherent assumption of nuclear sphericity. An important

distinction involving the rotational properties of the ellipsoid must be made however. If the description of the nucleus as an axially symmetric ellipsoid is valid, then the nucleus is able to rotate as a whole about an axis. The angular momentum of this collective rotation is \vec{R} and the total nuclear angular momentum is $\vec{I} = \vec{R} + \vec{j}$ and for the ground state \vec{R} is perpendicular to the intrinsic nuclear symmetry axis. The nuclear Hamiltonian is $H_N = H_{\text{rot}}(R) + H_{\text{int}}(j)$ where the first term is the rotation kinetic energy due to collective rotation of the deformed nucleus and the second is the intrinsic energy of the nucleon moving in the deformed potential. The nuclear wave function is thus $|\Omega; I, M, K\rangle \sim D_{MK}^I \chi_\Omega$ where D is a rotation D function which characterizes the collective rotation and connects intrinsic angular momentum values to those in the lab frame, M is the projection of the total angular momentum I on the z axis of the lab frame, K is the projection of I on the body fixed symmetry axis z' and χ_Ω is the intrinsic single particle wave function.

The relation between the classical intrinsic ellipsoidal quadrupole moment Q' , obtained above, and that quadrupole moment as seen in the lab frame Q involves a term in the product of the D-functions $Q = \int D_{MK}^I D_{MK}^{I*} Q' d\tau$. Due to orthogonality rules of the D-functions the following expression is obtained [Eder-68, Chapter 21]

$$Q = \frac{3K^2 - I(I+1)}{(I+1)(2I+3)} Q'.$$

for the ground state $K = I$ so the observed quadrupole is

$$Q_{(\text{obs})} = \frac{I(2I-1)}{(I+1)(2I+3)} Q'. \quad (2.17)$$

The significance of this expression is that the D-function provided the link between a quantity measured with respect to the body's symmetry axis and a quantity defined in the lab frame. The factor $I(2I-1)/(I+1)(2I+3)$ gives the projection of Q' on the lab fixed axis along which I has the projection M .

Next we shall discuss the single particle solution for motion in a distorted well given by Nilsson [Nils-55] so as to develop expressions for the magnetic moment; later we shall return to the consideration of the quadrupole.

The Hamiltonian is given by

$$H = H_0 + C\vec{l}^2 + D\vec{l} \cdot \vec{s}.$$

As was the case in the shell model the terms in C and D introduce the strong spin orbit interaction and "round" the bottom of the harmonic oscillator well. The only difference is that now the harmonic oscillator term is chosen to be anisotropic. The term H_0 is parameterized by a deformation parameter δ viz:

$$H_0 = \frac{\hbar^2}{2M} \nabla^2 + \frac{M}{2} (\omega_0^2 (1 + \frac{2}{3}\delta) (x^2 + y^2) + \omega_0^2 (1 - \frac{4}{3}\delta) z^2) \quad (2.18)$$

where distances x , y and z define the intrinsic nuclear coordinates. Rewriting H_0 to more clearly display the deformation dependence of H_0 , Nilsson obtains:

$$H_0 = \overset{\circ}{H}_0 + H_\delta = \hbar\omega_0 \frac{(-\nabla^2 + R^2)}{2} - \delta\hbar\omega \frac{4}{3} \sqrt{\frac{\pi}{5}} R^2 Y_2^0.$$

where $R^2 = x^2 + y^2 + z^2$, and $x^2 = \frac{M\omega_0}{\hbar} x^2$ etc. The first term is spherically symmetric and the second represents the coupling of the particle to the axis of deformation which is parallel to z . The Hamiltonian is diagonalized in a basis $|N\ell\Lambda\Sigma\rangle$ in which the operators $\overset{\circ}{H}_0$, ℓ^2 , ℓ_z and s_z are themselves diagonal with eigenvalues $(N + \frac{3}{2})\hbar\omega_0$, where N = total number of oscillator quanta, $\ell(\ell+1)$, Λ and Σ respectively. Now $\ell_z + s_z = j_z$ and correspondingly the quantum number $\Omega = \Lambda + \Sigma$ is introduced; further since j_z^{\dagger} commutes with the total Hamiltonian, Ω is a constant.

The wave function of the nucleon moving in the distorted well is $\chi_\Omega = \sum_{\ell, \Lambda} a_{\ell\Lambda}(\delta) |N\ell\Lambda\Sigma\rangle$. At zero deformation groups of the Nilsson orbitals coincide with the shell model levels and, as δ increases, the shell model state in effect splits into $j + \frac{1}{2}$ deformed orbitals. At very large values of δ , contributions from C and D appearing in the Hamiltonian are negligible and each state can be labelled by Ω , the parity and the triad $[N, n_z, \Lambda]$ where n_z is the number of quanta along the deformation axis.

The magnetic moment predicted by the Nilsson model is found by evaluating the magnetic moment operator

$\vec{\mu}_{op} = \mu_N (g_S \vec{s} + g_\ell \vec{\ell} + g_R \vec{R})$ where use has been made of equation 2.7. The additional term $g_R \vec{R}$ is the contribution to the magnetic moment caused by the collective circulation of the Z protons. The collective motion of the nucleus is viewed as a kind of 3rd orbital angular momentum with an averaged g -factor $g_R \approx Z/A$. The magnitude of the magnetic moment μ is found by noting that $\mu = \frac{\mu_{op} \cdot \vec{I}}{I+1}$. Nilsson obtains for the ground state moment

$$\mu = \frac{\mu_N I}{I+1} \left\{ g_\ell I + g_R + \frac{1}{2} (g_S - g_\ell) \left(\sum_{\ell} a_{\ell, K-1/2}^2(\delta) - a_{\ell, K+1/2}^2(\delta) \right) \right\}. \quad (2.19)$$

For the case of $K = 1/2$ there is an additional term involving a parameter which measures the amount of coupling between the collective rotation and the single particle motion, thus violating the assumption that $|\Omega, I, M, K\rangle$ could be given as product wave function. This need not concern us in this work however.

If it is assumed that the nucleons retain their free g -factors, then lines akin to the Schmidt limits can be drawn. Once again, the observed moments deviate from their "limits" indicating the importance of configuration mixing effects. After investigation of several deformed nuclei it was found that better agreement usually results if one uses reduced values for intrinsic spin g -factors g_s , so that for odd neutron nuclei the choice is $g_{s, eff} = 0.6 g_{s, free}$ [Borg-69]

Returning to the quadrupole moment it is noted that properly $Q = Q_{sp} + Q_{core}$ where Q_{sp} is the contribution of the single particle moving in the anisotropic well. However since typically $Q_c \gg Q_{sp}$ the latter can safely be neglected. Recalling that the equation for the intrinsic quadrupole moment is given (in terms of δ) by,

$$Q' = 0.8 Z R_0^2 \delta \left(1 + \frac{2}{3}\delta + \dots\right) \quad (2.20)$$

where R_0 is the charge radius of the nucleus, $R_0 = 1.2 \times 10^{-13} A^{1/3}$ cm. Combining this equation with projection factor (equation 2.17) the collective deformation is, in terms of observed quadrupole moment for $A \approx 150$:

$$\delta \approx \frac{3}{4} \left(-1 \pm \sqrt{1 + \frac{8}{3} \frac{Q'}{0.8ZR_0^2}}\right) \approx \frac{Q'}{0.8ZR_0^2}$$

where the positive sign has been adopted. Thus

$$\delta \approx \left(\frac{1}{0.8ZR_0^2}\right) \frac{(I+1)(2I+3)}{I(2I-1)} Q_{obs}$$

where Q_{obs} is the observed quadrupole moment in barns.

CHAPTER III

HYPERFINE STRUCTURE

In order to measure nuclear moments use is made of the hyperfine structure interaction (hfs) whose origin is the electro-magnetic coupling of the nuclear charge and current distributions with the magnetic and electric fields and gradients at the nucleus set up by the atomic electrons. Typically these fields and gradients are larger than those easily obtainable in the laboratory, and they are therefore exploited as a kind of natural resource which generates interactions that are large enough to permit easy observation. Because hfs depends on both nuclear and electronic contributions it does not provide the means for a direct determination of the nuclear moments. In the case of the nuclear magnetic moment direct determination is possible through techniques such as NMR or triple resonance. However the higher order moments do not admit themselves to direct determination. It turns out that important corrections, or at least allowances for possible uncertainties, must be made for moments determined through the hfs interaction. These corrections primarily centre about uncertainty in the electronic wave function.

Since the hfs "levels" can be characterized by an angular momentum quantum number these levels exhibit Zeeman splitting when subjected to an external magnetic field. The elucidation of the hfs constants, and in turn the nuclear moments, is effected through measurements of the separation of these magnetic sub-states.

A. Atomic Hamiltonian

The Hamiltonian describing the free atom is the sum of 3 terms, viz:

$$H = H_{\text{nuc}}(I) + H_{\text{elec}}(J) + H_{\text{hfs}}(F). \quad 3.1$$

The first of these terms, $H_{\text{nuc}}(I)$, was discussed in Chapter II and gives the nuclear contributions. The electronic contribution is represented by $H_{\text{elec}}(J)$, where J is the total electronic angular momentum quantum number. The eigenstates and eigenvalues of $H_{\text{elec}}(J)$ and solutions to the Schrödinger equation $H_{\text{elec}}(J) \psi = E_J(nlk)\psi$. In the electronic case the self-consistent field yields states which are usually appropriate to the L-S coupling scheme. Such states are denoted by the expression $^{2S+1}L_J$ where S is the coupled spin $\vec{S} = \sum \vec{S}_i$, L is total orbital angular momentum ($\vec{L} = \sum \vec{l}_i$) and $\vec{J} = \vec{L} + \vec{S}$. For n equivalent electrons the term value for the ground state can be found by application of Hund's rules which are based on general considerations concerning the overall symmetry of the electronic wave function and the repulsive nature of the inter-electron potential.

The third term, $H_{\text{hfs}}(F)$, is the hfs Hamiltonian and forms the centre of our interest. The quantum number F is a result of the electron-nuclear coupling effected by the hfs interaction and F is given by the vector equation $\vec{F} = \vec{I} + \vec{J}$.

Typically the energies corresponding to changes of a nuclear state or an electronic state are much larger than those due to $H_{\text{hfs}}(F)$, and so I and J are taken to be good quantum numbers.

B. Magnetic Dipole Interaction

Let us assume that the nucleus can be represented as a point mass. The magnetic field at the origin, or at the point nucleus, due to an orbital atomic electron is given by

$$\vec{H}_O = - \frac{e(\vec{V} \times \vec{r})}{r^3} + \frac{\vec{\mu}_e r^2 - 3\vec{r}(\vec{\mu}_e \cdot \vec{r})}{r^5} \quad (3.2)$$

where $\vec{\mu}_e$ is the intrinsic electron moment and \vec{r} is a vector joining the origin and the electron. Substitution of the orbital and intrinsic angular momenta, \vec{l} and \vec{s} yields

$$\vec{H}_O = - 2 \mu_O \frac{(\vec{l} - \vec{s} + 3\vec{r}(\vec{s} \cdot \vec{r})/r^2)}{r^3} \quad (3.3)$$

where μ_O is the Bohr magneton = $\frac{e\hbar}{2mc}$. Since the interaction energy of a magnetic dipole in a magnetic field is $W = -\vec{\mu} \cdot \vec{H}$ the magnetic hfs Hamiltonian is the sum

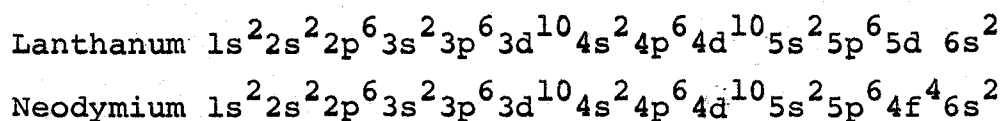
$$H_{\text{hfs}}^{\text{mag}} = - \sum_i \vec{\mu}_I \cdot (\vec{H}_O)_i \quad (3.4)$$

where $(\vec{H}_O)_i$ is the field at the origin due to the i^{th} non-s electron. The s-electrons have a finite probability amplitude at the origin and to account for this an additional term is added to (3.4) so that [Nier-57]

$$H_{\text{hfs}}^{\text{mag}} = \sum_{\substack{i \\ \ell \neq 0}} \vec{\mu}_I \cdot (\vec{H}_O)_i - \sum_{\ell=0} \frac{16\pi}{3} \frac{\mu_I}{I} \mu_O |\psi_i(0)|^2 \vec{I} \cdot \vec{J} \quad (3.5)$$

Each electronic sub-shell can only accommodate $2(2\ell+1)$ electrons - otherwise the Pauli principle would be violated.

For a filled sub-shell half the electrons have spin up and these $2\ell+1$ spin-up electrons have accounted for all the magnetic quantum numbers. The other half have spin down and, again, they range through all the $2\ell+1$ m_ℓ -values. Assuming that both spin groups have the same radial distribution an exact cancellation of the fields takes place and the sum in (3.5) need only be taken over electrons in unfilled shells. For the cases of interest here, $^{147,149}_{60}\text{Nd}$ and $^{140}_{57}\text{La}$, the ground configurations are



and, even though lanthanum does have a large amount of unpaired 6s electrons admixed from the configuration $(5d^2 6s)$ (see Section D)) we presently assume that there are no unpaired s-electrons. Thus

$$H_{\text{hfs}}^{\text{mag}} \equiv a_\ell \sum_i \vec{N}_i \cdot \vec{I} \quad (3.6)$$

where $a_\ell = 2\mu_N \frac{\mu_I}{I} \langle r_e^{-3} \rangle$ and μ_N is the nuclear magneton $= \frac{e\hbar}{2M_p c}$ where M_p is the proton mass. The vector operator \vec{N}_i characterizes the field at the point nucleus located at the origin, and $\langle r_e^{-3} \rangle$ is the expectation value of the inverse cube of the electron radius. The matrix elements of $H_{\text{hfs}}^{\text{mag}}$ are diagonal in the total atomic angular momentum $\vec{F} = \vec{I} + \vec{J}$. Calculation in the basis $|JIF\rangle$ yields [Wybn-65]

$$\langle JIF | H_{\text{hfs}}^{\text{mag}} | JIF \rangle = \frac{1}{2} hAK = W_{M1}$$

where $K = F(F+1) - J(J+1) - I(I+1)$

and

$$hA = 2\mu_N \frac{\mu_I}{I} \frac{\langle r_e^{-3} \rangle \langle J || \Sigma \vec{N}_i || J \rangle}{\sqrt{J(J+1)(2J+1)}}$$

For all isotopes the atomic factors $\langle r_e^{-3} \rangle$, $\langle J || \Sigma \vec{N}_i || J \rangle$, etc. remain constant and the following relationship (Fermi-Segrè formula) applies between isotope 1 and isotope 2,

$$\frac{A_1}{A_2} = \left(\frac{\mu_I}{I}\right)_1 \cdot \left(\frac{I}{\mu_I}\right)_2. \quad (3.8)$$

For the case of both an unpaired s-electron and n electrons with $l \neq 0$ Wybourne [Wybn, op cit] shows that

$$W_{M1} = \frac{hK}{4J(J+1)} [A\{J(J+1) + J_1(J_1+1) - s(s+1)\} + a_s\{J(J+1) + s(s+1) - J_1(J_1+1)\}] \sim \mu_I (c_1 + c_2) \quad (3.9)$$

where a_s is the s-electron hfs constant, $a_s = \frac{16}{3} \pi \mu_o \frac{\mu_I}{I} |\psi_s(0)|^2$.

In the above formula J_1 is the angular momentum to which the non-s-electrons couple, and J is the total electronic angular momentum so that $J = J_1 \pm \frac{1}{2}$. The important point is that the hfs interaction is still directly proportional to the nuclear moment μ_I .

These relations hold only for point nuclei and

indeed departures from equation (3.8) have been observed where both the A's and μ_I 's have been measured independently. This departure is known as the hfs anomaly and will be discussed in section D of this chapter.

C. Electric Quadrupole and Higher Order Interactions

In addition to a magnetic field, the atomic electrons also create an electric field gradient at the nucleus. It will prove useful to relax the assumption that the nucleus is a point and so the electric hfs interaction may be written as

$$H_{\text{hfs}}^{\text{elec}} = \int_{\tau_e} \int_{\tau_n} \frac{\rho_e \rho_n}{|\vec{r}_e - \vec{r}_n|} d^3\tau_e d^3\tau_n \quad (3.10)$$

where the ρ 's are the electronic and nuclear charge densities and \vec{r}_e and \vec{r}_n are radius vectors to infinitesimal volume elements of the electron cloud and nucleus, respectively. An expansion of the term $1/|\vec{r}_e - \vec{r}_n|$ is now made in terms of spherical tensors of rank k , viz:

$$\frac{1}{|\vec{r}_e - \vec{r}_n|} = \sum_k \frac{r_n^k}{r_e^{k+1}} (C_e^{(k)} \cdot C_n^{(k)}) \quad (3.11)$$

where it has been assumed that $r_n < r_e$. When the integration over the nuclear co-ordinates is carried out, the terms in the sum represent the energies of the various electric multipole moments, E_k^{μ} .

It was shown in Chapter II that the only non-zero values for E_k^{μ} are for even k . If $k=0$, then $H_{\text{hfs}}^{\text{elec}}$ is the Coulomb operator and its contributions have been taken into account in the electronic Hamiltonian $H_{\text{elec}}(J)$. However because of the finite size of the nucleus the assumption that $r_n < r_e$ for all values of the integration in (3.10) is not

quite true in general. This consideration manifests itself by the presence of isotope effects whereby all the atomic energy levels are shifted. As far as the hfs splittings are concerned, it only alters the zero of energy and not the separations between the levels themselves.

The $k=2$ term is the electric quadrupole interaction. The matrix elements of $H_{\text{hfs}}^{\text{elec}}$ for $k=2$ are given by:

$$\begin{aligned} \langle JIF | H_{\text{hfs}}^{\text{elec}} | JIF \rangle &= -e^2 (-1)^{J+I+F+2} \begin{Bmatrix} J & J & k=2 \\ I & I & F \end{Bmatrix} \\ &\times \langle J || r_e^{-3} c_e^{(2)} || J \rangle \langle I || r_n^2 c_n^{(2)} || I \rangle = \quad (3.12) \\ &= e^2 Q \langle r_e^{-3} \rangle \left(\frac{3/4 K(K+1) - I(I+1)J(J+1)}{2I(2I-1)J(2J-1)} \right) \langle J || c_e^{(2)} || J \rangle. \end{aligned}$$

where Q is the nuclear quadrupole moment, $K = F(F+1) - J(J+1) - I(I+1)$, and the expression in curly braces is a 6-j symbol which keeps track of the components in the coupling $I+J \rightarrow F$. Traditionally, one defines the electric quadrupole interaction constant B by $hB = e^2 Q \langle r_e^{-3} \rangle \langle J || c_e^{(2)} || J \rangle$. As was the case for the magnetic interaction constant A , the following ratio holds for isotopes 1 and 2 of a given element.

$$\frac{B_1}{B_2} = \frac{Q_1}{Q_2}. \quad (3.13)$$

The 6-j symbol in equation 3.12 has the property that it vanishes unless the elements of each of the triads (I, I, k) ,

(J,J,k) and (I,J,F) can form a triangle. One consequence of this rule is that the nuclear quadrupole moment (k=2) would not be observable if $J=1/2$ even though the nucleus could indeed possess a non-zero intrinsic quadrupole moment. Schwartz [Schw-55] has shown that a similar rule holds for any order k so that one can only observe multipoles up to order k such that $k = \text{lesser of } 2I \text{ or } 2J$. This restriction harks back to the result of Chapter II where the nuclear moments of order k had to satisfy $k \leq 2I$. If $I \geq 3/2$ then it is possible that the nucleus possesses a non-zero magnetic octupole moment. In addition, if $J \geq 3/2$ is also satisfied, there is a magnetic octupole hfs interaction which has been written by Schwartz (op cit) as

$$W_{M3} = \mu_0 \mu_I \frac{R_n^2}{r_e^5} \times E(\ell, J) N(I, g_s, g_\ell)$$

where R_n is the nuclear radius, r_e is electronic orbital radius and $E(\ell, J)$ is a function of the electronic quantum numbers ℓ and J while $N(I, g_s, g_\ell)$ is a function of the nuclear spin I and the nuclear spin and orbital g-factors g_s and g_ℓ . Assuming that $E(\ell, J)$ and $N(I, g_s, g_\ell)$ are of order unity it is possible to estimate the size of the octupole interaction relative to that of the dipole interaction

$$\frac{W_{M3}}{W_{M1}} \sim \frac{\mu_0 \mu_I R_n^2 / r_e^5}{\mu_0 \mu_I / r_e^3} = \frac{R_n^2}{r_e^2} \approx 10^{-6}$$

Because of the smallness of the octupole interaction its contributions to H_{hfs} can be very safely neglected in the work reported here.

In the same way, other higher order hfs interactions are negligible. Thus, combining the results of this and the previous sections, we have the hfs interaction given by

$$W_F^O = \frac{1}{2} hAK + hB \frac{[\frac{3}{4} K(K+1) - I(I+1)J(J+1)]}{2I(2I-1)J(2J-1)} \quad (3.14)$$

D. Hyperfine Structure Anomaly

If the above description of the hfs interaction were complete then the Fermi-Segrè relation, eq. 3.8, would hold exactly. Thus independent measurements of A and μ_I , for any two isotopes, 1 and 2, of a particular element would always satisfy $\frac{A_1}{A_2} = \frac{I_2}{I_1} \frac{(\mu_I)_1}{(\mu_I)_2}$. In fact Murphy's fifth law prevails and the Fermi-Segrè relation must be amended by the inclusion of a correction term.

It is useful to re-write the Fermi-Segrè relation as $\frac{A_1}{A_2} = \frac{I_2}{I_1} \frac{(\mu_I)_1}{(\mu_I)_2} (1 + {}_1\Delta_2)$ where ${}_1\Delta_2$ is called the hfs anomaly. For very light nuclei, ${}_1\Delta_2$ can be attributed to changes in electron radial term r_e^{-3} due to the centre of mass moving in as the neutron number increases. For heavy elements, such as Nd and La, the anomaly is due to the finite size of the nucleus.

In section B we assumed that the nucleus was a point dipole. In fact the finite nuclear size causes a smearing out of the nuclear moment [Bohr-50].

In order to calculate the hfs energy $H_{\text{hfs}}^{\text{mag}}$ the interaction is split into the sum of two integrals - one from the origin to the nuclear "edge" and the other from the nuclear surface out to ∞ . Bohr and Weisskopf specifically assumed a uniform charge distribution in the nucleus. The electronic wave function is described using the Dirac equation. Because only s and $p_{1/2}$ electrons wave functions have non-zero values at the origin, only configurations involving unpaired s or

$p_{1/2}$ electrons should show appreciable effects. For these type electrons, Bohr and Weisskopf find ${}_1\Delta_2 \leq 0.7-1.0\%$ with the anomaly becoming larger with increasing Z . Stroke et al [Strk-62] have extended the calculation to allow for a trapezoidal nuclear charge distribution in keeping with the electron scattering experiments of Hofstadter and co-workers [Hofs-63]. The contributions to ${}_1\Delta_2$ from the spin and orbital g -factors are calculated using the configuration mixing approach of Noya et al. [op cit.] Such an approach means that Stroke et al are able to calculate ${}_1\Delta_2$ for specific shell model states. Typically, for the cases tested, they found ${}_1\Delta_2 \leq 0.2\%$ which was in good agreement with experimental results known to those authors. For distorted nuclei, Reiner [Rein-59] used pure Nilsson orbitals and a uniform nuclear charge distribution to find a possible anomaly of ${}_1\Delta_2 \leq 2\%$.

Recently Vanden Bout [Vand-67] measured ${}_1\Delta_2 \approx 8\%$ for ^{197}Au and ^{198}Au ! Part of the reason that the anomaly is so large in odd-odd nuclei is because both protons and neutrons can sum their separate anomalies to the odd-odd moment. Large anomalies are not limited to Au isotopes either; Mössbauer spectroscopy has shown an hfs anomaly of 7% for ^{193}Ir (73 keV state) in comparison with ^{193}Ir ground state (Peri-69).

The electronic ground doublet for $_{57}\text{La}$ is $^2D_{3/2,5/2}$. Using atomic energy levels M.S. Freed of the Argonne group [Chil-69] has calculated

$$|{}^2D_{3/2,5/2}\rangle \approx .90|(5d6s^2) {}^2D_{3/2,5/2}\rangle + .45|(5d^26s) {}^2D_{3/2,5/2}\rangle.$$

That is, the observed lanthanum ground doublet is really a mixture of two electron configurations*. This degree of mixing is consistent with Ting's measurement of the A values for ^{139}La which showed $A_{5/2}:A_{3/2} = 1.29$ and not 3.3 as predicted by equation (3.7). This mixing means that the observed A's are really the sum of contributions due to equations (3.7) and (3.9). In view of the 8% anomaly observed in ^{198}Au , we estimate that the hfs anomaly for ^{140}La compared to ^{139}La could be possibly as large as $(.45)^2 \times 8\% \sim 1.5\%$ due to the admixture of the state $|5d^26s {}^2D_{3/2,5/2}\rangle$.

For the case of neodymium isotopes, comparison of the hfs splitting constants $A_{J=4}$ for ^{143}Nd and ^{145}Nd with their moments determined by triple resonance reveals $1\Delta_2 \approx 1/2\%$ [Smit-65, Pend-63] even though there is no sizable admixture of unpaired s or $p_{1/2}$ electrons in the ground multiplet. Because ^{149}Nd is apparently a distorted nucleus and thereby may possess a quite different distribution of nuclear magnetism than that found in ^{145}Nd , we allow a 2%

* Other terms are present too but they do not have nearly the amplitude of the term from $5d^26s$.

uncertainty in determining μ_I from A.

Another small correction to μ_I results from the fact that when an external field H_0 is applied to an atom, the electrons set up a diamagnetic field which reduces the external field by an $-\sigma H_0$. Thus the true moment is $\frac{1}{1-\sigma}$ the apparent moment. The shielding factor σ has been calculated and is accepted to have only a 5% error [Full-60]. The calculated values of σ are given by Kopfermann [Kopf-58] and are typically 1-2%.

E. Sternheimer Correction

Electronic configuration mixing is responsible for a large contribution to A in the case of lanthanum. The configuration interaction is also responsible for large corrections in the value of Q derived from B. The most famous case involves ^{65}Cu and the breakdown of equation (3.12). Measurements of B in the states $3d^{10}4p$, $^2P_{3/2}$ and $3d^94s^2$ $^2D_{5/2}$ yield $Q = -.161(3)$ and $-.228(5)$ barns respectively. Similarly Murakawa has shown that discrepancies also exist among various electronic states of ^{139}La [Murk-58, Murk-61].

In a series of papers Sternheimer has considered the effects of core polarization on the quadrupole coupling constant B. [Ster-59, Ster-67]. The nuclear quadrupole moment Q induces a distortion of the core electrons. Thus, the electric field gradient is altered and is no longer calculable by equation (3.12). The electron core distortion is treated as a perturbation $H_1 = -\frac{Q(3\cos^2\theta-1)}{2r^3}$, and the matrix elements of H_1 are evaluated for certain appropriate electronic states. In general the only non-vanishing contributions of H_1 are the so-called angular excitations $n\ell \rightarrow n\ell \pm 2$ and the radial excitations $n\ell \rightarrow n'\ell$. Since electronic wave functions have to be anti-symmetrized there are both direct and exchange terms for the angular and radial excitations. Excitations of the type $n\ell \rightarrow n\ell \pm 2$ are characterized by an angular rearrangement which tends to concentrate the electrons

in regions of minimum potential, which are near the poles of the nuclear symmetry axes for $Q > 0$. This concentration causes the quadrupole constant B to be decreased from the unperturbed value ($H_1 = 0$) and hence the effect is one of shielding. On the other hand, the radial excitations $n\ell \rightarrow n'\ell$ tend to enhance (anti-shield) the value of B compared to the unperturbed case. The exchange terms are of opposite sign to the direct terms and thus angular-exchange leads to enhancement of B and radial-exchange leads to shielding of B .

Sternheimer's results are summarized by the equation $Q = Q_{app} (1-R)$ where Q_{app} is the apparent quadrupole moment - apparent because the perturbation H_1 has induced either shielding or anti-shielding of the true quadrupole moment, Q . Because the final value of R depends on the sum of the angular and radial contribution for direct and exchange terms no general conclusions can be drawn about R until all effects are included. For copper, Sternheimer finds $(1-R_{4p})/(1-R_{3d}) = 1.43$, in excellent agreement with the ratio, 1.42(5), of the measured values of Q measured in the 4p and 3d states of ^{65}Cu . This agreement is felt to be an overwhelming triumph of the Sternheimer calculation.

Sternheimer has also found that for the 5d states of Pr and Tm $R_{5d} = -0.38$ and -0.44 , respectively. The average value is in good agreement with Murakawa's results

for B in various atomic states of ^{139}La . This value for R will be adopted in the analysis of the present lanthanum results. Sternheimer also finds that $R_{4f} = +0.2$. Such a result has been confirmed by measurements in rare earth salts [Ster-67, Hufn-65], but has not yet been verified for free atoms. Nevertheless it will be used in the analysis of the neodymium results.

F. Zeeman Effect

In order to determine the hfs constants atoms of the substance under investigation are subjected to a steady, uniform, and weak magnetic field so that the hfs "levels" split up into their magnetic sublevels in accord with the Zeeman effect. The separations between these sub-levels, which depend on the constants A and B, are found from the frequency of applied rf field required to induce transitions between the sub levels. The theory of these induced transitions will be discussed in the next section. The present section deals with the Zeeman effect itself.

The Hamiltonian describing the interaction of an atom with a constant magnetic field \vec{H} is

$$H_{\text{mag}} = -\vec{H} \cdot (\vec{\mu}_J + \vec{\mu}_I) = -\mu_0 \vec{H} \cdot (g_J \vec{J} + g_I \vec{I})$$

where μ_0 is the Bohr magneton and g_J is the electronic g-factor $g_J = \frac{\mu_J}{J\mu_0}$, g_I is the nuclear g-factor $= \frac{\mu_I}{I\mu_0}$ which is of order $g_J/2000$. Because of the negative charge of the electron μ_J is negative and so $g_J < 0$. Assuming that I and J are constant, the atomic Hamiltonian for an atom in a magnetic field becomes

$$H = H_{\text{hfs}} - \vec{H} \cdot (\vec{\mu}_J + \vec{\mu}_I). \quad (3.15)$$

The hfs interaction couples \vec{I} and \vec{J} to form the total angular momentum F. Using the well known angular momentum

operators the matrix elements of H_{mag} can be calculated.

Allowing the direction of H to define the z axis, the matrix elements of H_{mag} are:

$$\langle F, m_F | H_{\text{mag}} | F, m_F \rangle = H m_F (\alpha(J, I, F) g_J + \beta(J, I, F) g_I) \quad (3.16)$$

$$\langle F', m_F | H_{\text{mag}} | F, m_F \rangle = H m_F (g_I - g_J) \gamma(J, I, F) ; F' = F - 1 \text{ only}$$

$$\text{where } \alpha(J, I, F) = - \frac{\mu_0}{2F(F+1)} (F(F+1) + J(J+1) - I(I+1))$$

$$\beta(J, I, F) = - \frac{\mu_0}{2F(F+1)} (F(F+1) + I(I+1) - J(J+1))$$

$$\gamma(J, I, F, m_F) = \frac{\mu_0}{2F} \sqrt{\frac{(F-I+J)(F-J+I)(F+I+J+1)(I+J-F+1)(F^2 - m_F^2)}{(2F-1)(2F+1)}}$$

where m_F denotes one of the $2F+1$ Zeeman sublevels. It is to be noted that the matrix elements of H_{mag} are diagonal in m_F because of the axial symmetry of the applied field.

For weak magnetic fields we can treat terms in H_{mag} as a perturbation on the hfs interaction energy, thus:

$$W_{F, m_F} = W_F^0 + \langle F, m_F | H_{\text{mag}} | F, m_F \rangle + \sigma(H^2)$$

where W_F^0 is the hfs energy given by (3-14). In very strong fields ($H \geq 10^4$ G), the interaction energy of the electronic dipole moment with the applied field becomes comparable to the hfs splittings, so that the nuclear and electronic moments are no longer coupled. The splittings are then calculated in an $|I m_I, J m_J\rangle$ basis. In this scheme the

hfs sub levels are at energies given by:

$$W_{m_I, m_J} = m_J m_I hA + hB \frac{(3m_I^2 - I(I+1))(3m_J^2 - J(J+1))}{4IJ(2J-1)(2I-1)} \quad (3.17)$$

Because of the decoupling, I and J and their magnetic quantum numbers m_I and m_J enter symmetrically. Due to the large field the diagonal terms:

$$\langle m_I, m_J | H_{\text{mag}} | m_I, m_J \rangle = \mu_0 H (g_J m_J + g_I m_I)$$

are typically much larger than the hfs terms and so the latter are treated as perturbations in the strong field limit.

Restricting ourselves to only first order perturbation theory, the structure of the magnetic sub-level can be obtained from the weak field and strong field expressions. Interpolation between these limits and application of the principle that levels having identical values of m_F never cross leads to a schematic drawing of the energy levels as in Figure (3.1).

Here, in the weak field region, the hyperfine levels are split into $2F+1$ equally spaced components in accordance with eq. (3.16).

In the strong field region, the levels split into groups determined by m_J , having a slope $-\mu_0 m_J g_J / h$ MHz/gauss. Within an m_J group, the projections of the nuclear spin m_I are ordered in accordance with the hfs splitting term (3.17).

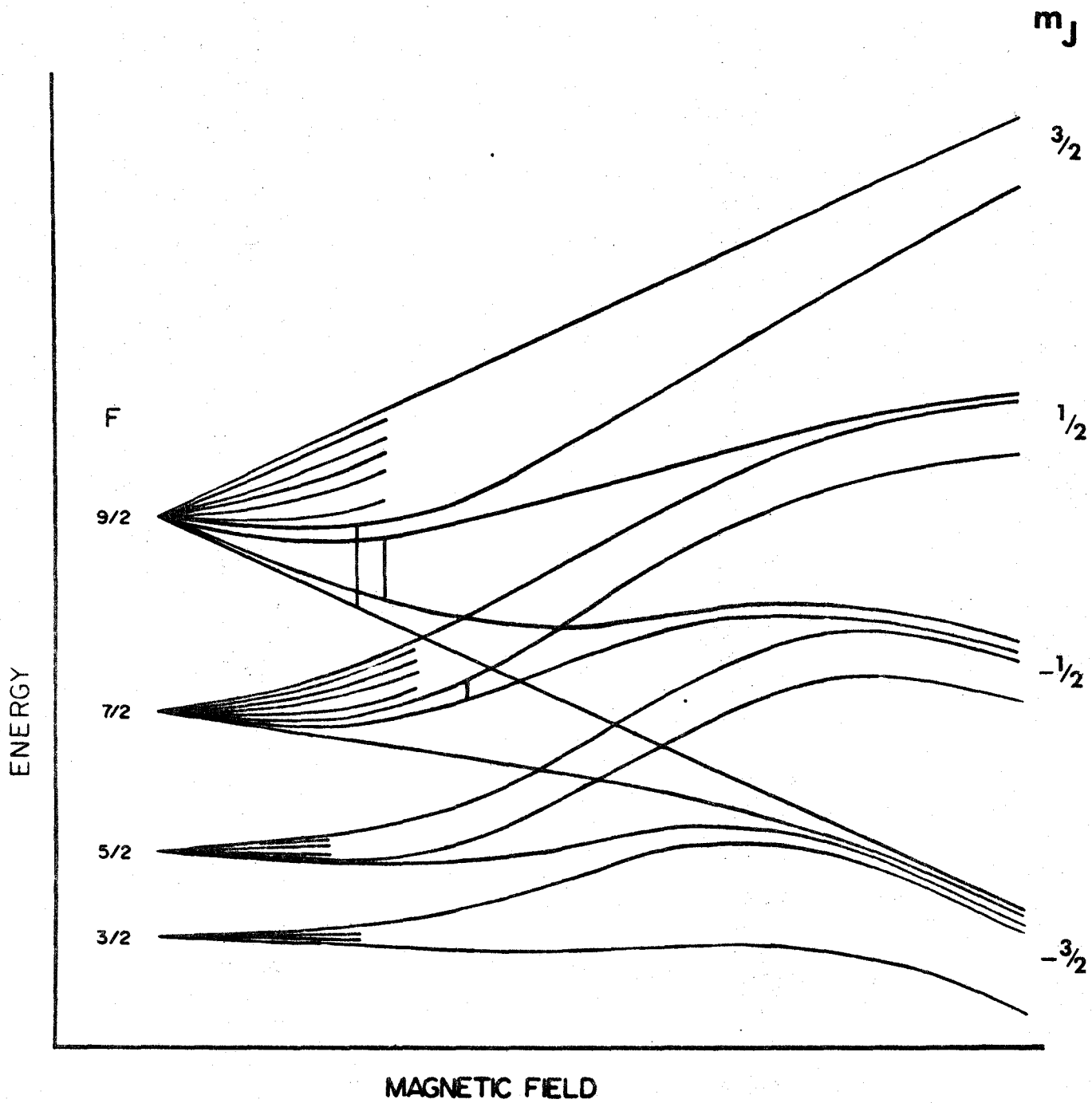
Because of the de-coupling the strong field region is analagous to the Paschen-Back effect of atomic spectroscopy.

With the general features of the energy level diagram established, consideration is now paid to the determination

Fig. 3.1 ZEEMAN SPLITTING OF A hfs MULTIPLET

For weak field each hfs level is split into $2F+1$ equally spaced levels. For very strong fields \vec{I} and \vec{J} decouple and have a slope $\Delta W_{mF} / H = \frac{g_J \mu_0}{h} m_J \text{ MHz/gauss.}$

Hence they are split into groups determined by m_J .



$$W_{F,m_F} = W_{F,m_F}(l, j, A, B; g, H)$$

of the hfs constants A and B from the Zeeman splittings. For illustration it is sufficient to consider only second order terms in H

$$W_{F,m_F} = W_F^0 + \alpha(I,J,F) H g_{J,m_F} + \sum_{F'=F\pm 1} \frac{H^2 \gamma^2 (g_J - g_I)^2}{W_F^0 - W_{F'}^0} \quad (3.18)$$

where use has been made of equation (3.16). Because of the difference $W_F^0 - W_{F'}^0$, in the denominator, the departure of W_{F,m_F} from a linear dependence on magnetic field provides a measure of A and B. One way of measuring these departures, is to induce transitions between the magnetic substates of a hyperfine multiplet. The details will be discussed in the next section.

G. Induced Magnetic Dipole Transitions

The hfs constants A and B may be determined by measuring the frequency required to induce transitions between the Zeeman levels of a hfs multiplet. In the experiments reported here, an oscillating r.f. field is applied perpendicular to the static field (C field) which is along the Z-axis. Thus $\vec{H}_{rf} = H_0 \cos(\omega t) \hat{i}$ and the r.f. Hamiltonian is

$$H_{r.f.} = -\vec{\mu} \cdot \vec{H}_{rf} = -\frac{1}{4} \{ \mu_0 H_0 (g_J - g_I) (J_+ + J_-) + g_I (F_+ + F_-) \} (e^{i\omega t} + e^{-i\omega t}). \quad (3.19)$$

The raising and lowering operators J_{\pm} and F_{\pm} have been used to express the x components of I and J.

For non-zero C field, F is no longer a good quantum number and a state of a hfs multiplet is given by a sum over all states F having a component m_F , $|(F)m_F\rangle = \sum_{F'} a_{F'}(m_F) |F'm_F\rangle$, where label (F) indicates the level from which the state evolved. The $a_{F'}$ are found from solution of the eigenvector problem - equation 3.15. Thus, at non-zero values of C-field,

$$\langle (F')m'_F | H_{rf} | (F)m_F \rangle = \hbar b (e^{i\omega t} + e^{-i\omega t}) \times \sum_{F', F''} a_{F'}(m'_F) a_{F''}(m_F) \alpha(F', m'_F; F, m_F)$$

where

$$b = \frac{\mu_0 H_0 (g_J - g_I)}{4(2I+1)} \quad \text{and} \quad \alpha(F', m'_F; F, m_F) =$$

$$\langle F', m'_F | (2I+1) (J_+ + J_-) + \frac{(2I+1)g_I}{g_J - g_I} (F_+ + F_-) | F, m_F \rangle$$

In this investigation, we are only concerned with transitions of the type $F' = F$. Also, because the mixing of states $|F' \neq F, m_F\rangle$ into $|F, m_F\rangle$ is very small in a weak field, we write

$$\alpha_{m, m'} \equiv \sum_{F, F'} \alpha(F', m'_F; F, m_F) a_{F', (m'_F)} a_F(m_F) \approx \alpha(F, m'_F; F, m_F).$$

Consider the two-level case in which the allowed states are $|1\rangle$ and $|2\rangle$, and assume that, at $t=0$, the atom is in state $|1\rangle$. The matrix to be solved is

$$\begin{pmatrix} W_1 & \hbar b \alpha_{12} e^{i\omega t} \\ \hbar b \alpha_{21} e^{-i\omega t} & W_2 \end{pmatrix}$$

where the counter-rotating components $e^{-i\omega t}$ associated with $\langle 1|H|2\rangle$, and $e^{+i\omega t}$ associated with $\langle 2|H|1\rangle$, have been dropped. This is necessary in order to make it possible to formulate certain analytic expressions required to calculate the MQT probabilities. In any event, their contribution to the transition probability is small since they involve $\frac{1}{\omega + \omega_0}$ rather than $\frac{1}{\omega - \omega_0}$ [Bloc-40]. If the perturbation is applied for a time τ the transition probability is [Rabi-37]

$$P_{1 \rightarrow 2} = \frac{(2b)^2}{(\omega_0 - \omega)^2 + (2b)^2} \sin^2\left(\frac{1}{2} \sqrt{(\omega_0 - \omega)^2 + b^2} \tau\right). \quad (3.20)$$

where $\omega_0 = \frac{W_1 - W_2}{\hbar}$ and ω is the angular frequency of the applied r.f. field. We note that the transition probability

is 100% if $\omega = \omega_0$ and if $b = \frac{n\pi}{\tau}$ ($n=1,2,\dots$). The resonance line shape is governed predominantly by the Lorentzian

$f(x) = \frac{1}{1+x^2}$ and the r.f. amplitude dependence is $\frac{\partial P}{\partial b}(\omega=\omega_0) \approx b^2$ for very small b .

A multiple quantum transition (MQT) is one of type $|Fm_F\rangle \rightarrow |Fm_F \pm n\rangle$ where $n > 1$. Because of the selection rule for H_{rf} , $m_F' = m_F \pm 1$, an n -quantum transition takes place by the absorption or stimulated emission from the rf field of n separate quanta. Using a perturbation theory approach, Salwen [Salw-55] and, independently, Hack [Hack-56] showed that the transition probability for an n -quantum transition has the same form (Lorentzian in frequency) as equation (3.20)

$$P_{m',m} \approx \frac{b^2_{m',m}}{(\omega_{m',m}^* - \omega)^2 + b^2_{m',m}} (\sin^2(n\pi \sqrt{(\omega_{m',m}^* - \omega)^2 + b^2_{m',m}} \tau)) \quad (3.21)$$

$$n = |m' - m|.$$

where $\omega_{m',m}^*$ is the angular frequency which corresponds to the resonance intensity peak. In fact

$$\omega^* = \omega_0 + \left(\frac{b}{n}\right)^2 \left(\sum_{i=m-1} \frac{|\alpha_{i,m}|^2}{\omega_{m,i} - \omega_{m',m}} + \sum_{i=m+1} \frac{|\alpha_{i,m}|^2}{\omega_{m',m} - \omega_{m,i}} \right.$$

+ similar terms for m').

The term ω_0 is the "generalized Bohr frequency" given by

$$\omega_0 = \frac{W_{F,m} - W_{F,m'}}{|m - m'|n} \quad W_{F,m} > W_{F,m'}$$

That is, ω_0 represents a kind of compromise frequency which is used to connect the levels m', m through the $(n-1)$ intermediate states of the Zeeman multiplet. Because of the $(b/n)^2$ -term in ω^* there is a shift in the nominal frequency ω_0 due to the perturbing field. If such shifts are large, then corrections allowing for those shifts should be made. The rf field parameter $b_{m',m}$ is defined by

$$b_{m',m} = \frac{2}{n} b^n \frac{\alpha_{m,i} \alpha_{i',i} \dots \alpha_{i^{(n-1)},m'}}{(\nu_{m,m'} - \nu_{m',i}) (\nu_{m,m'} - \nu_{m',i'}) \dots (\nu_{m,m'} - \nu_{m',i^{(n-1)}})}$$

The frequency denominators, $(\nu_{m,m'} - \nu_{m',i})$ measure the departure of the levels of a Zeeman multiplet from equal spacing and thus their product, which appears as the denominator of $b_{m',m}$, grows very rapidly as the C-field increases. For large fields, vastly larger r.f. amplitudes are required to achieve sizeable transition probabilities than would be required at very small fields when the energy levels are nearly equally spaced. Also, because of the factor n in the probability expression (3.21) and in its role in $b_{m',m}$ the full width at half maximum for MQT is only $\frac{1}{n}$ times the width for a single quantum transition (equation 3.20). Indeed this narrowing of MQT is observed in the experiments reported here.

Salwen's perturbation theory results are only taken

to 2nd order in b . But, because of the large b values required to excite MQT some question may be raised as to the validity of boldly applying Salwen's formula for ω^* to see if serious frequency shifts occur which would require correction. A non-perturbation theory solution which uses exact diagonalization of H_{rf} has been reported elsewhere [Pier-66]. Using the methods developed there, the expected frequency shifts were calculated for the transitions observed in ¹⁴⁰La. It was found that, for the r.f. field amplitudes required to maximize the transition probability, the peaks of the resonances were shifted only 1 or 2 kHz from the nominal MQT frequencies - an amount which is entirely negligible.

In practice, far more serious shifts of the frequency peak can occur due to inhomogeneities of the C-field [Happ-64]. These shifts can be either positive or negative depending on the concavity, as evidenced by the second derivatives $\frac{\partial^2 H}{\partial x^2}$, of the C-field intensity profile. Broadening of the resonance line shape beyond the width given by the uncertainty principle, $\Delta\nu \sim 1/\pi\tau$, is also symptomatic of field inhomogeneity. Great care must be taken, therefore, to ensure that in each run the field inhomogeneities have been eliminated or, at least, minimized. This procedure will be discussed later.

In summary, an oscillating field of the type defined by equation (3.19), can induce transitions of the type $|F, m'\rangle \rightarrow |F, m\rangle$ so that, if $|m' - m| > 1$ an n-quantum transition is induced. Calculation reveals that these transitions are narrow, $\text{FWHM} \sim 1/n$ (FWHM the single quantum transition), and require a lot of r.f. power for their excitation. Even at these large r.f. amplitudes, however, only very small frequency shifts from "nominal" frequency ω_0 are expected.

It is also possible for the r.f. field, (3.19), to excite transitions of the type $|F, m\rangle \rightarrow |F \pm 1, m \pm 1\rangle$, that is, transitions between the sub levels of different hfs multiplets. Such transitions are called "direct" transitions in contrast to the "Zeeman" transitions. Observation of direct transitions permits very accurate determination of the hfs constants A and B.

CHAPTER IV

THEORY OF EXPERIMENT AND EXPERIMENTAL RESULTS

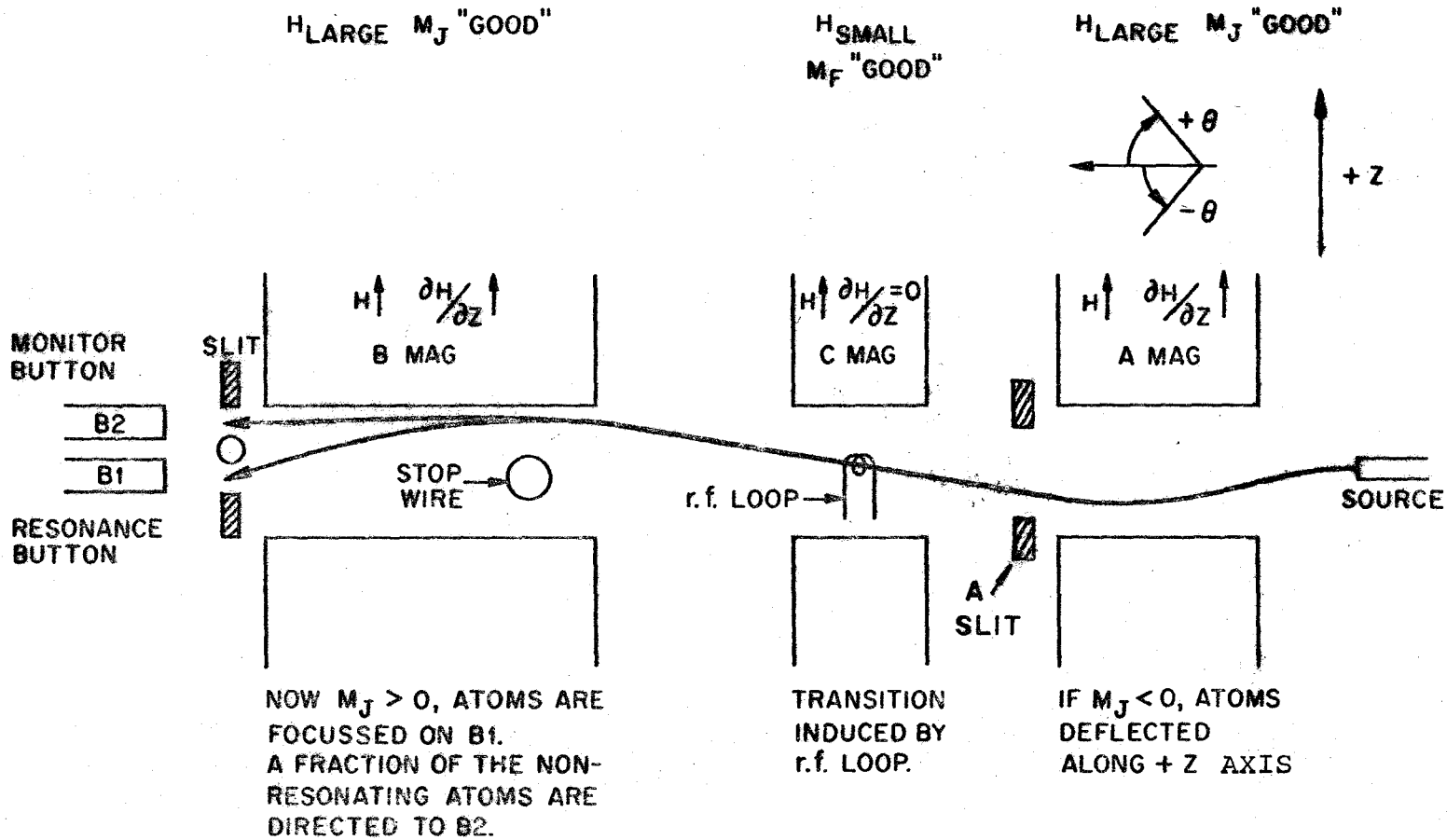
The atomic beam apparatus has been described in detail elsewhere [King-60, Came-62] and, accordingly, only those aspects of its operation important to the interpretation of the experimental results will be discussed here. In addition the results of the experiments performed will be given in this chapter.

A. Operation of the Apparatus

The source material is evaporated from a small tantalum oven and emerges through a slit to form an atomic beam. Figure 4-1 shows the layout. The apparatus is under a vacuum of approximately 10^{-6} Torr to prevent beam scattering. The atoms of the beam, in their nearly 1-meter journey along the x-axis are subjected to three regions of magnetic field. The fields of the A- and B-magnets are strong and inhomogeneous and their field directions and gradients are parallel to each other but perpendicular to the beam direction. Because the fields are strong ($H \sim 10^4$ G) it can be assumed that \vec{I} and \vec{J} are completely decoupled. The magnetic energy is $W_{\text{mag}} = -\vec{\mu}_J \cdot \vec{H} - \vec{\mu}_I \cdot \vec{H} \equiv -\mu_0 g_J m_J H$ where $g_J < 0$ and the direction of \vec{H} has been taken to define the z-axis. The

Fig. 4.1 APPARATUS

The trajectory of the focussed atoms is indicated schematically. The locations of the collimating slits and the buttons are also shown.



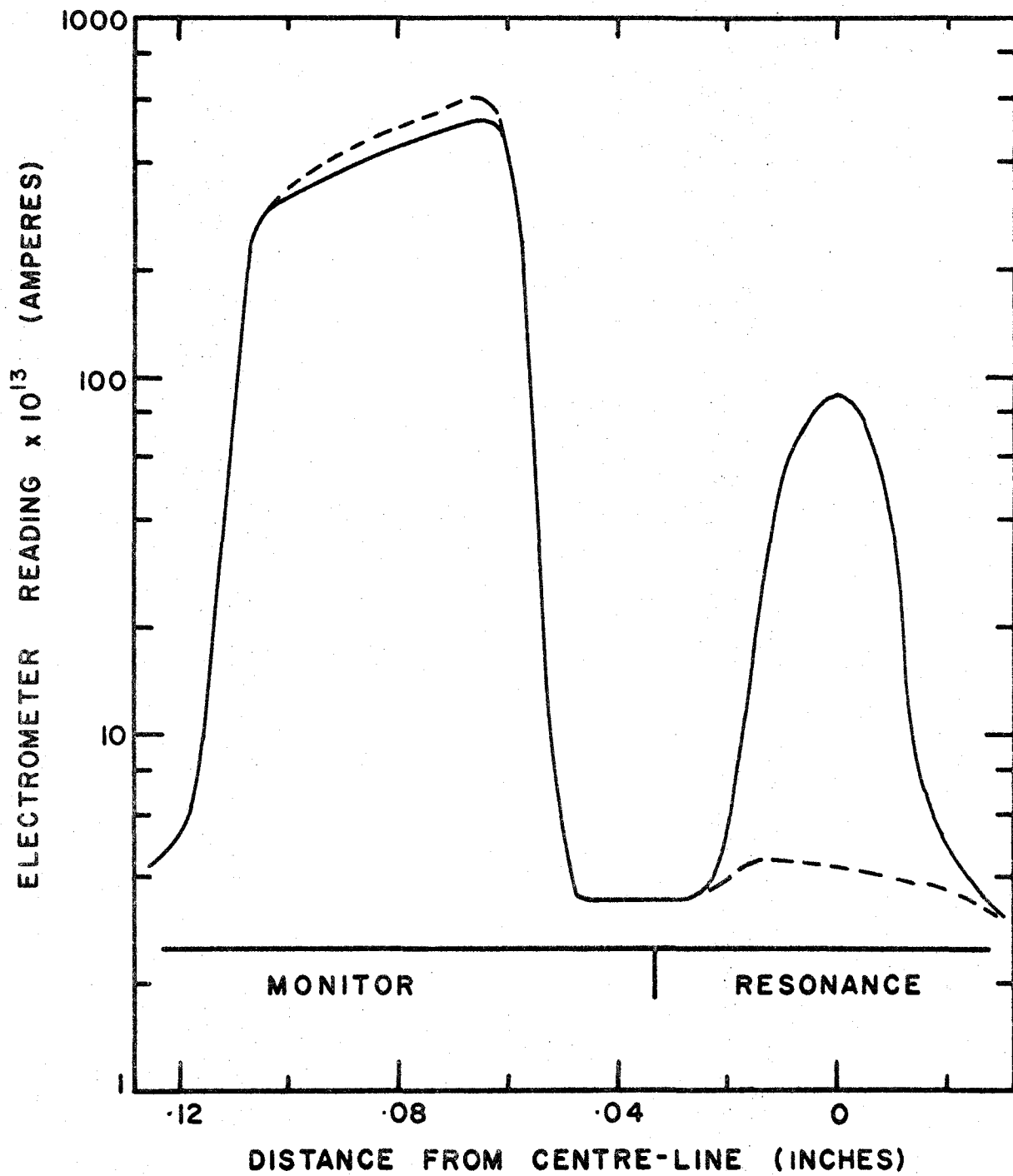
force on the atoms due to the gradient is

$$\vec{F} = -\nabla W_{\text{mag}} = \frac{\partial H}{\partial z} \mu_0 g_J m_j \hat{k}.$$

Therefore atoms having $m_J > 0$ and initially emerging at a positive angle θ are deflected towards the apparatus axis. Similarly atoms having $m_J < 0$ and emerging at negative θ are deflected back towards the apparatus axis. All other atoms are, in principle, deflected away from the axis and miss the collimating slits and are lost. Those atoms moving too fast to be deflected or those having $m_J = 0$ are blocked from reaching the exit slit by the stop wire. In the B-field, atoms are deflected (again) in the same direction as they were in the A-field region, and thus miss the exit slit. If, however, the sign of m_J has changed between the A and B regions, then the atom is subjected to a kind of restoring force by the B-field and is refocused so that it can pass the exit slit and land on the resonance button. The requisite sign change of m_J is effected by inducing a transition between the original magnetic substate $|F m_F\rangle$ and another $|F' m_F'\rangle$. A hot wire or surface ionization detector is mounted behind the buttons. The current generated by beam atoms becoming ionized and boiling off the tungsten wire is amplified by an electrometer. The mount is capable of being swung in an arc so that different regions of the beam can be intercepted. This mobility is very useful during the alignment procedure. Figure 4-2 shows the exit beam profile taken with the hot wire.

Fig. 4.2 EXIT BEAM PROFILE

The resonance and monitor components of the beam are shown. The data is for ^{133}Cs but the shape is preserved for all atoms having $J > 0$. The dashed lines correspond to the profile obtained with no rf inducing field applied.



The hot wire is also used to find the frequency peaks of the calibrating resonances in ^{39}K . Discussion of the calibration procedure will take place later in section D.

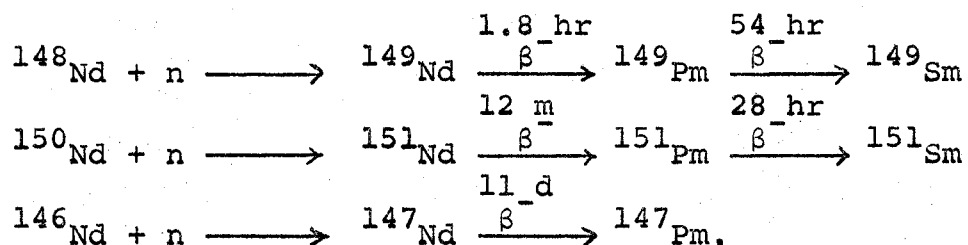
Atoms of ^{147}Nd , ^{149}Nd and ^{140}La are radioactive and undergo β^- decay. The number of atoms deposited on the button is indicated by the button's activity. The buttons are counted using low background β -counters which are shielded from cosmic rays by the use of anti-coincidence circuits in conjunction with hemispherical guard tubes surrounding the inner tubes.

The runs themselves are conducted in the following way: The C-field is set to some predetermined value using resonances in ^{39}K . After allowing time for magnet stabilization, and subsequent field calibration (again, of course, using the ^{39}K beam), the radioactive beam is raised (like Lazarus) and pairs of buttons, one "resonance" and one "monitor" are loaded into the apparatus. Loading is accomplished through the use of a button bar. A channel cut into its base permits the insertion of a pair of buttons, side by side, when the bar is out of the vacuum case. The bar is then advanced through two stages of pump-down and finally brought to rest with the buttons behind the exit slits. After depositing for 10 to 15 minutes, the buttons are changed for another pair and a new r.f. frequency is set. While the second pair is being exposed, the first

pair is counted and the ratio of their activities, resonance-to-monitor, is noted. Any changes in exposure time can be made as may be required by observing the monitor counting rate.

An increase in the ratio of the counting rates at a particular frequency means that transitions which reverse the sign of m_J are being induced at that frequency. Proceeding in this way a resonance can be traced out and presented as a plot of relative activity against applied frequency.

Neutron irradiation of natural neodymium metal can be summarized by the following reactions:



Thus to facilitate the ${}^{149}\text{Nd}$ experiments an automatic counting system was installed. This action was taken because the presence of the radioactive promethium isotopes in the beam (the vapour pressure of Pm is close to that of Nd) obscured the ${}^{149}\text{Nd}$ activity thereby masking the ${}^{149}\text{Nd}$ resonances.

The outputs from the eight β^- counters were fed to scalars which were slaved to a master timer-scaler that

allowed the scalers to accumulate counts for some predetermined time interval. At the end of the interval on command from the master timer-scaler the contents of each of the scalers was read out and printed on a teletype. After the contents of the last scaler in the chain had been printed the scalers were re-zeroed and the process repeated. In this way decays could be followed for several half lives and the amount of ^{149}Nd activity identified.

Table 4.1 lists the pertinent apparatus components used in these experiments. It will be noted that several of the components listed were "built, designed and perfected" by the author's esteemed colleague, Mr. R.G.H. Robertson. It is a pleasure to acknowledge his substantial contribution to this work.

TABLE 4.1

Electronic Equipment

<u>Item</u>		<u>Description</u>
Magnet Supplies for A,B, and C Magnets	Designed, built and perfected by R.G.H. Robertson	Transistorized, current Regulated. A & B Supply capable of 1.5 A into $10^3 \Omega$. C supply can be varied continuously to produce fields from 0 to 300 G. Stability is ≈ 1 part in 10^5 over 4 hours.
Electrometer	Designed, built and perfected by R.G.H. Robertson	Sensitivity (FSD) is 10^{-14} A.
Automatic oven temperature control and supply	Designed, built and perfected by R.G.H. Robertson	Oven is kept at constant temperature by controlling filament current so that product of emission current and accelerating voltage is a constant. Arc protection via SCR's. Capable of 1000 V at 500 mA.
Frequency Counter	Hewlett Packard Model 5246L	0-3 GHz via suitable plug-in units. Long term stability is 1 part in 10^7 .
Rf Signal Generators	Wandel and Golterman Model LMS-68 and LO Series plug-in units	Range 4-1,000 MHz via plug-in units. Maximum Rf output is 1/2-1 watt into 60Ω
Rf-amplifier	Boonton Radio Corp. Model 230A	Range 10-500 MHz. Output is nominally 4 watts into 50Ω
Automatic Counting System	Canberra Industries 10-Blind Scalers Model 1476, Timer Scaler Model 1493, Blind Scaler Display Model 1477 Teletype Scanner Model 1488, Teletype console Model 33 ASR	Prints out, at preselected time intervals, the contents of up to ten scalers.

B. Computer Programmes

Several computer programmes have been written to facilitate these investigations. The first of these, written by R.G.H. Robertson and called FCALC, prints out the frequencies of all focussable transitions for a given choice of H, A, and B. The programme finds these frequencies by diagonalizing the atomic Hamiltonian H (eq.3.15).

After several resonances have been observed the programme LOLA is used to calculate, for different combinations of A and B, the residuals between the experimentally observed frequencies and those predicted at the appropriate fields for the particular transitions assumed. The results of all the observed resonances are combined by calculating

$$\chi^2 = \sum_{i=1}^N \frac{(v_i - v_{i,obs})^2}{(\sigma_i)^2}$$

where v_i is the frequency calculated for the i^{th} resonance, $v_{i,obs}$ is the experimentally observed frequency of the i^{th} resonance and σ_i is its error. Resonances in different J states can be combined with each other if the ratios $A_{J'}/A_{J''}$ and $B_{J'}/B_{J''}$ are known for at least one isotope of the element under investigation. The values of A and B which minimize χ^2 are adopted as the experimentally determined values.

In essence the programmes LOLA and FCALC are different versions of the same programme. However, because they were written independently they served as verification that, indeed, both programmes are correct. This was done by comparing their results for specific values of the input constants. So as to rule out the presumably unlikely possibility that both programmes were making the same mistake their results were also compared, for certain alkali atoms in their $J=1/2$ states, with the results of a programme which used the exact Breit-Rabi formula. Since the latter is a solution for the case of I or $J=1/2$, only a quadratic equation need be solved to find the eigenvalues of H . In all these tests the agreement was exact.

The programme MQT finds the optimum rf field amplitude for a given transition and choice of A , B and magnetic field H . When the optimum value has been found, the resonance line shape is printed out to reveal if a significant power shift will occur.

Finally, it was necessary in the ^{149}Nd experiments to separate the 1.8-hour ^{149}Nd activity on the buttons from the background activity due to 28-hour ^{151}Pm and 54-hour ^{149}Pm . This separation was done using the computer programme FIX which least-squares fits the observed decay of the activity to a two-component exponential growth and decay, thus

$$y(t) = A[e^{-\lambda_a t} + \frac{\lambda_c}{\lambda_a - \lambda_c} e^{-\lambda_c t}] + B e^{-\lambda_b t}$$

where the different background activity of the promethium isotopes are lumped together into a single pseudo-activity having a decay constant λ_b taken appropriate for a 36-hour half life. The initial amount of ^{149}Nd is given by A and the initial promethium activity is B. The term

$$\frac{\lambda_c}{\lambda_a - \lambda_c} e^{-\lambda_c t}$$

allows for that amount of long-lived activity which is specifically due to decay of ^{149}Nd to 54-hour ^{149}Pm . Here λ_c is taken appropriate to the half life of the daughter.

C. General Experimental Considerations

1. The Plan of the Experiments

At low field, the resonance frequency of any Zeeman transition can be accurately predicted when J , g_J , H , I and F are known. This is implied by the linear term in the perturbation expansion, equation (3.18). Thus any given resonance can be found at low field in spite of one's ignorance of the values of the h.f.s. constants. At higher field, the quadratic terms in H , whose denominators are functions of the hfs intervals, cause the observed frequencies to depart from a linear dependence on field. In general, the frequency shift is

$$\delta\nu = \nu_{\text{lin}} - \nu_{\text{obs}} = \frac{C_1 H^2}{C_2 A + C_3 B}$$

where C_1 , C_2 and C_3 are known. Obviously, the shift may be determined with greater and greater accuracy as the field is increased. Measuring $\delta\nu$ in two F-states permits the evaluation of two independent linear combinations of A and B , resulting in a unique solution for them. Additional measurements in other F-states makes an over-determination possible.

Ideally, the hfs constants would be determined by measuring the hfs intervals using direct transitions (i.e. $\Delta F = \pm 1$, $\Delta m_F = 0, \pm 1$) at low field.

For the lanthanum and neodymium atoms reported here, it turns out that these transitions would be practically impossible to observe. With several values of J and relatively large nuclear spins, the beam intensity is distributed among a great number of separate quantum states. Thus, any effect which acts to increase the resonance height becomes important.

Under fairly broad assumptions, it can be shown [Rams-56, King-60] that the transmission (I/I_0) of the apparatus is given by

$$I/I_0 \approx 1 - e^{-v_c^2/\alpha^2} \quad (4.4)$$

where $\alpha = \sqrt{\frac{M}{2kT}}$ is the most probable velocity in the oven at temperature T , and v_c is called the critical velocity of the apparatus. For $v \leq v_c$, all atoms passing through the collimating slits can be refocused by the magnets provided they undergo appropriate transitions. However, the faster moving atoms are not deflected enough to avoid the stop-wire. In fact, v_c^2 depends linearly on the field gradients, the g_J of the atoms and $|\Delta m_J|$ in the transition. For both lanthanum and neodymium, $(v_c/\alpha)^2$ is small with the present apparatus and so, from equation (4.4), the relative intensity of two transitions of different multiplicity becomes

$$\frac{I(\Delta m_J = \pm N)}{I(\Delta m_J = \pm 1)} \approx N.$$

The preferential focussing of multiple quantum transitions

over 1-quantum transitions forms an important experimental aid when investigating atoms with small g_J . Since direct transitions do not permit large multiplicity their resonances will be weak in comparison to the most favourable Zeeman resonances.

There is another circumstance which favours the observation of Zeeman transitions. In certain F-states, it is possible for transitions of several different multiplicities to be superimposed at the same frequency if the magnetic field is not too large. When this occurs, those resonances will be further augmented relative to resonances due to only a single transition.

These considerations were confirmed by experiments performed with a stable lanthanum beam and the hot-wire detector. The hfs constants for ^{139}La (99.9% abundance) have been accurately determined by Yu Ting [Ting-57] using the ABMR apparatus at N.R.C., Ottawa. Thus one can calculate that the following transitions in the $J=5/2$, $F=6$ state all occur at the same frequency, 14.164 MHz, in a 20G field:

$$\begin{array}{lll}
 m_F = -3 \leftrightarrow -4 & \Delta m_J = 1 & N = 1 \\
 -2 \leftrightarrow -5 & 3 & 3 \\
 -1 \leftrightarrow -6 & 5 & 5
 \end{array}$$

Other MQT in $F=6$ should be split off from each other by 0.030 MHz and are not superimposed. In the $F=4$ state, there is only a single $\Delta m_J = \pm 1$ transition. When these resonances and the direct hyperfine transitions were examined

it was found that the latter ($\Delta m_J = \pm 1$) were only about 1/10 as intense as the F=6, superimposed transitions. The search for the F=4 transition was unsuccessful. Thus, only if the corresponding superimposed resonances in ^{140}La were quite intense, i.e. if they were observed with a signal-to-background ratio of ~ 10 , could there be any hope of observing $\Delta m_J = \pm 1$ resonances. Similar considerations apply to the radioactive neodymium experiments.

2. Field Calibration

The C-field strength was calibrated by means of a ^{39}K beam detected on the hot wire at the beginning and end of each run. Two resonances were used, the one-quantum Zeeman transition $|2,-2\rangle \leftrightarrow |2,-1\rangle$ and the field dependent hyperfine transition $|2,2\rangle \leftrightarrow |1,1\rangle$. First it was established by plotting out the resonance line shape that the resonances were symmetrical and that the frequency of the peak did not shift when the rf voltage on the loop was increased by a factor of 5 or 10. If shifts did occur, implying an inhomogeneity, the C-field was de-gaussed, or simply raised and lowered, and the whole procedure repeated until no power shifts could be seen. The frequencies at the peaks of the two resonances were each taken ten times and the fields predicted from each group were averaged to provide the recorded field strength. The error assigned included the

extremes of both groups. In the same manner, the field was remeasured at the end of each run and the average of the initial and final values was adopted, viz.

$$\bar{H} \pm \delta H = \frac{H_{\text{init}} + H_{\text{fin}}}{2} \pm \frac{1}{2\sqrt{2}} (\delta H_{\text{init}} + \delta H_{\text{fin}}).$$

So as better to insulate the results against the effects of any possible systematic error and thereby to verify that the calibration procedure was valid, a separate series of tests was conducted using several calibrating beams. These beams were the alkalis ^{23}Na , ^{39}K , and ^{133}Cs whose properties are very well known. For some values of C-field the resonance frequencies for the calibrants were found and from these frequencies the field value was computed. The results were compared and it was found that within the error, good agreement always resulted. These runs were done for both strong and weak fields (~ 200 G and 20 G).

The same sort of experiment was carried out using the F=6 resonances in stable ^{139}La . Here the resonances were used to predict the value of g_J for the $J = 5/2$ of ^2D . This method of measuring g_J was possible because of Ting's precise measurements of $A_{5/2}$ and $B_{5/2}$ for ^{139}La , and because of Sheriff and William's determination of μ_I [Sher-51]. The resonances were observed at 75 and 125 G and use was made of a chart recorder to monitor the electrometer output while the oscillator slowly swept through a resonance. The results

of these runs were:

H (Gauss)	g_J	
75 (4 times)	-1.1985(9)	} $g_J = -1.1991(5)$
125 (4 times)	-1.1993(6)	

where the errors represent a standard deviation. This result should be compared with the very accurate value, $g_J = -1.19885(5)$ of Goodman and Childs [Good-68]. The agreement is quite satisfactory and confirms the assertion that there is no serious systematic error in the field calibration procedure.

3. The Radioactive Counting Procedure

In the experiments with the radioactive beams, the buttons were exposed to the beam for, typically, 10- or 15-minute periods which resulted in counting rates of about 300 c/min and 5 c/min on the monitor and resonance buttons, respectively. The buttons were first sprayed with a plastic lacquer (so as to prevent contamination of the counters) and then put into the counters. The monitor button and the resonance button were counted, in turn, in the same counter - thereby removing any dependence the results might have on relative counter efficiencies. Generally the buttons were counted until about 10^3 counts were recorded. Standard corrections for decay were made and the results were computed

as the resonance-to-monitor ratio

$$r = \frac{C_R - B}{C_M - B} \pm r \sqrt{\frac{1}{N_R} + \frac{1}{N_M}}$$

where C_R is the count rate for the resonance button and C_M is that for the monitor. The counter background is B (≈ 2 c.p.m.), and N_R and N_M are the total number of resonance and monitor counts respectively. Typically the relative error in r was $\approx 3\%$.

D. The ^{140}La Experiments

Samples of natural lanthanum, in the form of metal chunks sealed in evacuated quartz vials, were irradiated in the McMaster reactor. The purity of the material was verified by analyzing the resulting γ -spectrum. The only activity present in any significant amount was 40-hour ^{140}La , which was to be expected since the isotopic composition of natural lanthanum is 99.9% ^{139}La and 0.1% ^{138}La . The atomic beam sources, of about 20 milligrams, were irradiated for 20 hours to produce a specific activity of 10 mCi/mg.

After activation, the samples were loaded into a tantalum crucible which, in turn, was placed in a small tantalum atomic beam oven. The latter had a 0.010" slit and a total surface area of about one square inch. It was heated by electron bombardment at a constant power of 250 watts. Each sample would last for about 12 hours, thereby permitting the collection of about 50 exposures per source.

One troublesome feature of the project was the extremely intense γ -fields surrounding the samples, typically 5 to 10 r/hour at one meter. The hazardous aspect meant that the experiments had to be spaced out in time so as to reduce the radiation dosage to the author and his colleagues. Other measures included surrounding the oven-chamber end of the apparatus with lead blocks and self-enforcement of a rule never to try to make any required repairs to the oven

interlock or oven chamber within two weeks after a lanthanum run.

The major experimental difficulty, however, was in the production of a steady lanthanum beam. Beam instabilities showed up in two ways:

- (a) The beam intensity, as determined by the activity on the monitor button, could vary by a factor of two on occasion during a run even though the oven-heating power was kept constant throughout.
- (b) The rf-off background activity could vary by as much as a factor of four during the course of a run.

These two variations were apparently quite independent of one another and so the background could not be related to the monitor activity. Of course, the background fluctuations were of primary concern since the use of the double collection scheme compensated for beam intensity variations.

Resonances in stable ^{139}La were investigated for the purpose of optimizing the machine alignment to produce the best signal-to-background ratio for the ^{140}La resonances. It proved to be of crucial importance to very carefully secure the oven position since the background was very sensitive to oven placement. Therefore during the ^{140}La runs several exposures were taken initially with the rf turned off, moving the oven bar small distances in and out. The

position corresponding to minimum "rf-off" activity was picked and the experiment was then finally under way. Although this procedure minimized the severity of the background fluctuations by minimizing the background itself, it by no means eliminated the fluctuations. Thus it was necessary to take several more "rf-off" exposures during a run. A graph of these data was then plotted and the background during the resonance exposures was inferred by interpolation. The data for a typical run is shown in Figure 4.3. Also illustrated is the resulting resonance line shape after the background is subtracted.

The instabilities were probably due to surface diffusion of lanthanum through the exit slit of the oven and its subsequent evaporation from the outer surface. This evaporation has the effect of enlarging the source's extent in the Z direction far beyond the design parameters of the apparatus.

It has been stated already that two atomic states, $^2D_{3/2}$ and $^2D_{5/2}$, are present in the beam at the temperature used. Since $I = 3$ for ^{140}La [Pete-60] there are five different F-states in which focussable Zeeman transitions should occur; namely,

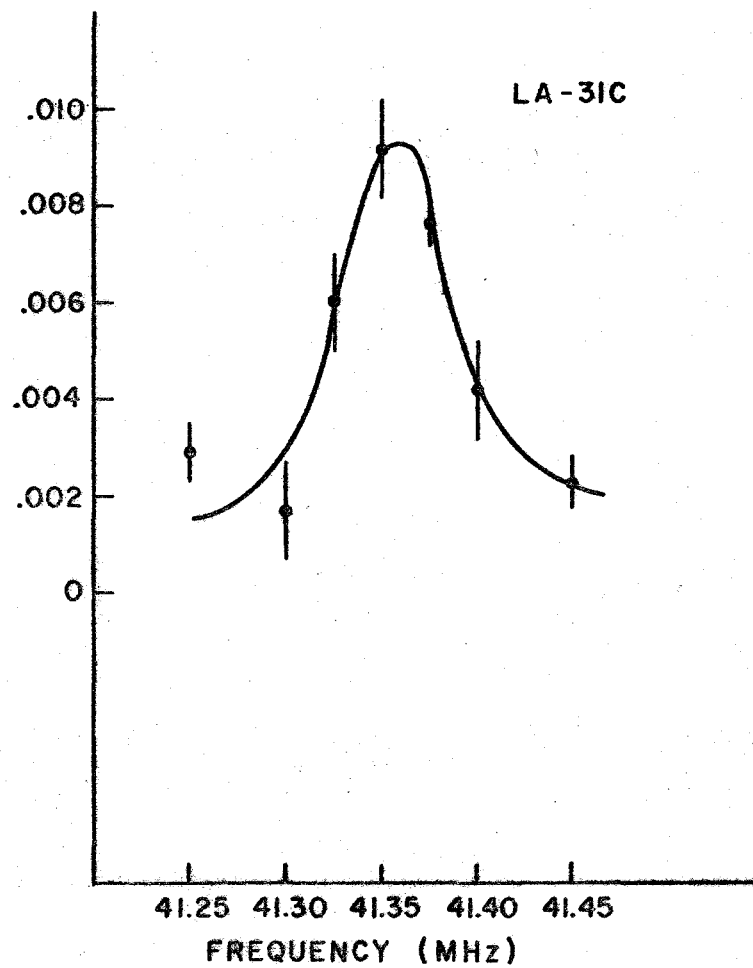
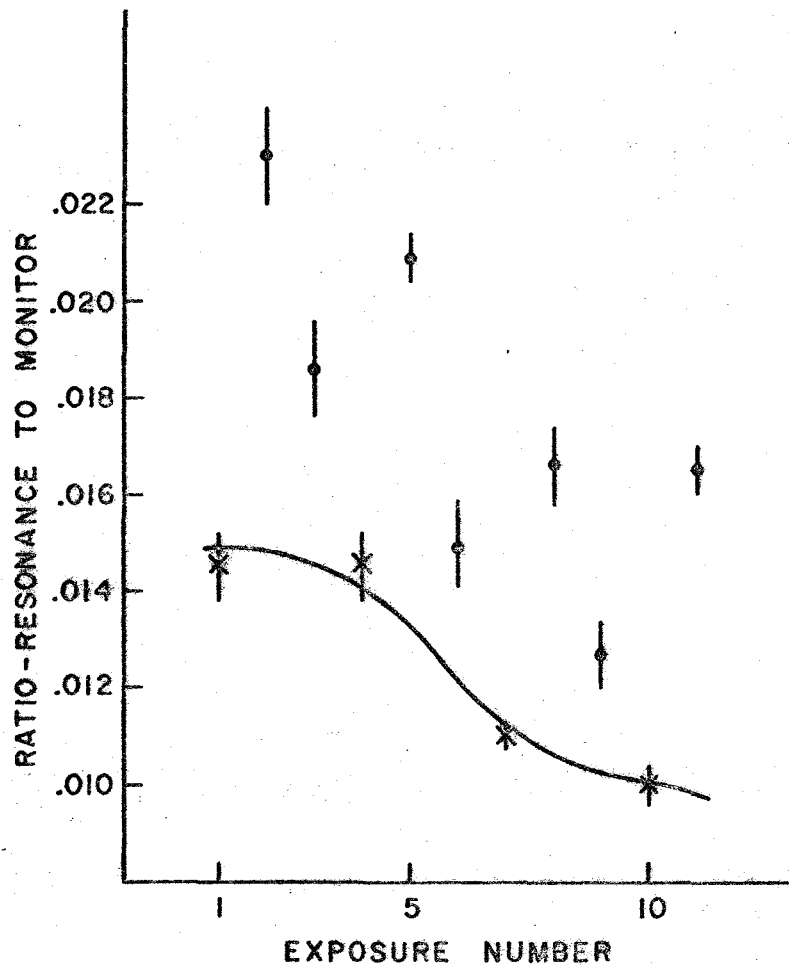
$$J = 3/2 \quad F = 9/2 \text{ and } 7/2$$

$$J = 5/2 \quad F = 11/2, 9/2 \text{ and } 7/2.$$

However, in the light of the discussion about the advantages

Fig. 4.3 BACKGROUND INTERPOLATION AND RESONANCE LINE
SHAPE (^{140}La)

On the left the raw data from a lanthanum run are presented. The background or rf-off exposures are indicated by the crosses. The resonance line shape on the right is the result of subtracting the interpolated background from the resonance exposures. This interpolated background is indicated by the solid line.



of observing superimposed MQT, the experiment was pretty much restricted to the observation of transitions of the type $\Delta m_J = \pm 3$ and ± 5 . It was decided, therefore, to search for the $F = 11/2$ and $9/2$ resonances in $J = 5/2$. By virtue of the relationships

$$\frac{A_{5/2}}{A_{3/2}} = 1.2902(1) \text{ and } \frac{B_{5/2}}{B_{3/2}} = 1.2106(6)$$

reported by Ting [Ting-57] for ^{139}La , the $J = 3/2, F = 9/2$ resonance served as a check.

To second order in H , the frequencies of the transitions are given by:

$$J = 3/2 \quad F = 9/2 \quad \Delta m_J = \pm 1, \pm 3 \quad \nu_{1,3Q} = 0.370 H + \frac{0.205 H^2}{\frac{9}{2}A_{3/2} + \frac{3}{4}B_{3/2}}$$

$$\Delta m_J = \pm 3 \quad \nu_{nQ} (n \geq 3) = 0.370 H + \left(\frac{9-n}{6}\right) \frac{0.205 H^2}{\frac{9}{2}A_{3/2} + \frac{3}{4}B_{3/2}}$$

$$J = 5/2 \quad F = 11/2 \quad \Delta m_J = \pm 1, \pm 3, \pm 5 \quad \nu_{1,3,5Q} = 0.763 H + \frac{0.420 H^2}{\frac{11}{2}(A_{5/2} + \frac{1}{10}B_{5/2})}$$

$$\Delta m_J = \pm 5 \quad \nu_{nQ} (n \geq 5) = 0.763 H + \left(\frac{11-n}{6}\right) \frac{0.420 H^2}{\frac{11}{2}(A_{5/2} + \frac{1}{10}B_{5/2})}$$

$$F = 9/2 \quad \Delta m_J = \pm 1, \pm 3 \quad \nu_{1,3Q} = 0.729 H + \left(\frac{0.760}{\frac{9}{2}A_{5/2}} - \frac{0.280}{\frac{11}{2}(A_{5/2} + \frac{1}{10}B_{5/2})}\right) H$$

$$\Delta m_J = \pm 3 \quad \nu_{nQ} (n \geq 3) = 0.729 H + \left(\frac{7-n}{4} \right) \left(\frac{0.760}{2^{A_{5/2}}} - \frac{0.280}{2(A_{5/2} + \frac{1}{10} B_{5/2})} \right) H^2$$

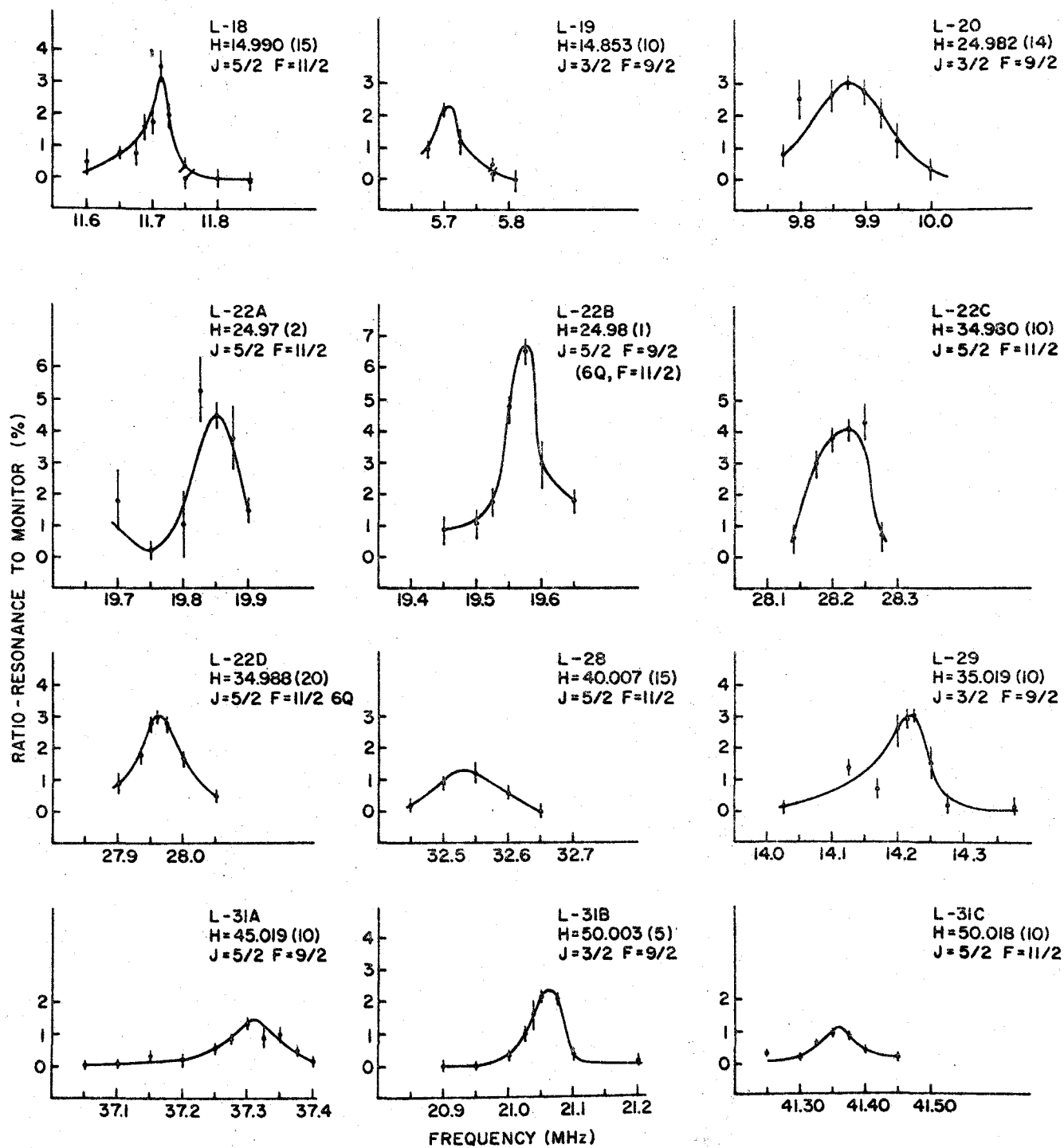
where ν , A_J and B_J are in MHz and H is in gauss. For the $F = 11/2$ transition, the 1-, 3- and 5-quantum transitions superimpose at the same frequency until the third order terms in H become large enough to split them apart. It turned out that this began to be significant at fields of about 60 G. The resonance in $J=5/2$, $F=9/2$ was very useful because it is quite insensitive to $B_{5/2}$.

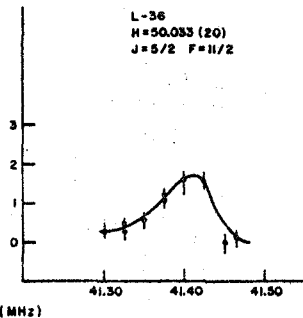
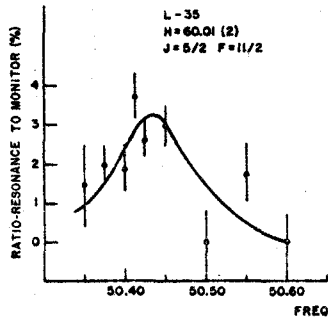
In all, 20 resonances were observed in ^{140}La , which represents the achievement of some 95 separate experiments. That is, only about one fifth of the experiments were successful. Of the 20 resonances, 2 were rejected - one at low field on the basis of gross disagreement with all the others, and one at 40G because of its distorted line shape. Figure 4-4 shows the 14, observed at higher fields, which were used in the calculation of the hfs constants, $A_{5/2}$ and $B_{5/2}$, by means of the programme LOLA.

Of course, that programme requires that each resonance be uniquely identified by initial and final quantum numbers. Because the third order splitting of the superimposed resonances was small compared to the line width at the fields used, resonances in $F = 11/2$ were assigned quantum numbers appropriate to the 3-quantum transition (whose predicted frequency is in between that for the 1Q and that for the 5Q transition). The resonances in $F = 9/2$ (for both J -values) were also treated as

Fig. 4.4 ¹⁴⁰La RESONANCES USED IN OBTAINING THE FINAL RESULTS

In these drawings, the vertical error bars primarily reflect the uncertainties in the background interpolation.





pure 3-quantum transitions - the argument being that these should represent the major contribution because of the preferential focussing of $\Delta m_J = \pm 3$ compared to $\Delta m_J = \pm 1$. To confirm the validity of this approach the data were also analyzed treating the transitions all as 1Q, and then all as 5Q or 3Q (as appropriate). There were no significant changes in the values of A and B at which the minimum χ^2 was found, although a slightly smaller χ^2 occurs for the 3-Q compromise fit.

For the χ^2 distribution, the standard deviation is $\sqrt{2f}$ where f is the number of degrees of freedom. We are fitting 14 resonances to two parameters so $f=12$. Figure 4.5 is a plot of χ^2 versus $A_{5/2}$ and $B_{5/2}$. The fact that $\chi_{\min}^2 \sim f/2$ indicates a somewhat conservative assignment of error in the frequency of each resonance. Noting that the displacement of either A or B by one standard deviation from its central value should increase χ^2 by $\sqrt{2(12)} \approx 5$, we find:

$$|A_{5/2}| = 55.9(4) \text{ MHz}$$

$$|B_{5/2}| = 38(4) \text{ MHz}$$

and

$$A_{5/2}/B_{5/2} > 0.$$

This means that hfs constants in ^{139}La and ^{140}La are related in the following way:

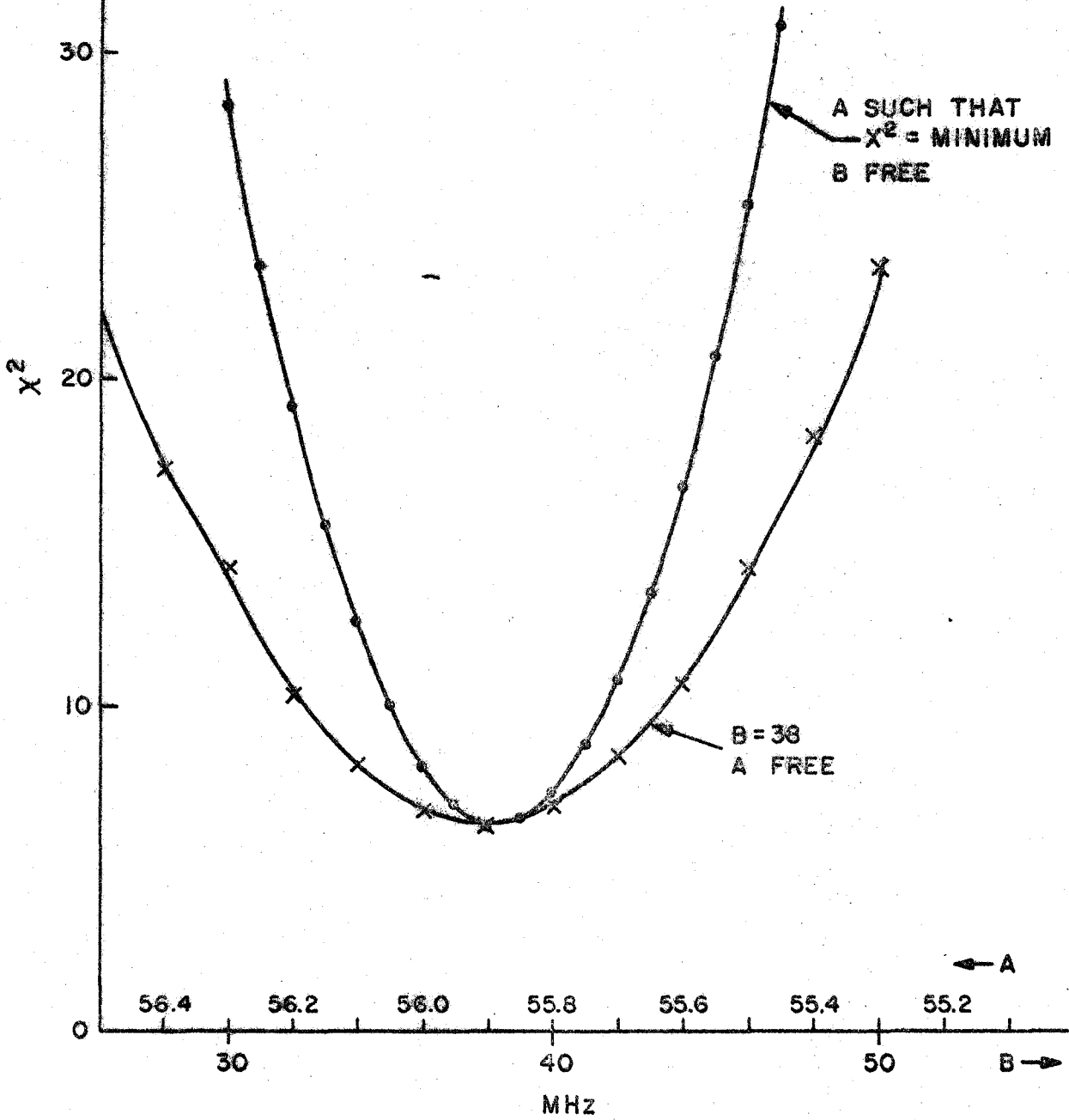
$$\frac{A_{5/2}^{140}}{A_{5/2}^{139}} = 0.307(2) \qquad \frac{B_{5/2}^{140}}{B_{5/2}^{139}} = 0.70(7).$$

Fig. 4.5 χ^2 AS A FUNCTION OF $A_{5/2}$ AND $B_{5/2}$ FOR ^{140}La

[12 DEGREES OF FREEDOM]

PLOT OF χ^2 VS. $A_{5/2}$ AT $B_{5/2} = 38$ MHz, AND

PLOT OF $\chi^2_{(min)}$ VS. $B_{5/2}$ $A_{5/2}$ SUCH THAT $\chi^2 = \text{MINIMUM}$



Of course, the hfs constants in the $J=3/2$ state were constrained to maintain the ratios observed in ^{139}La . No separate determination was possible here because only one Zeeman transition in $J = 3/2$ was investigated. Table 4.2 summarizes the data and also gives the individual residuals calculated for the adopted values of $A_{5/2}$ and $B_{5/2}$.

The nuclear moments for ^{140}La are found using the Fermi-Segrè formula

$$\mu_I^{140} = \frac{A^{140}}{A^{139}} \frac{I^{140}}{I^{139}} \mu_I^{139}$$

and

$$Q^{140} = \frac{B^{140}}{B^{139}} Q^{139}.$$

For the comparison isotope, the pertinent values [Sher-51, Ting-57] are

$$I^{139} = 7/2$$

$$\mu_I^{139} = +2.778(1) \text{ n.m.}$$

$$A_{5/2}^{139} = 182.1706(6) \text{ MHz}$$

$$B_{5/2}^{139} = 54.213(14) \text{ MHz.}$$

Ting reported $Q^{139} = +0.27(2) \text{ b}$, but he assumed a net Sternheimer shielding of the nuclear quadrupole moment given by $R_{5d} = +0.116$. In an extensive calculation, including both direct and exchange terms, Sternheimer [Ster-67] found that

TABLE 4-2

The ^{140}La Resonances

$ F, m_F\rangle \rightarrow F', m'_F\rangle$	ν_{exp} (MHz)	$\delta\nu_{\text{exp}}$ (MHz)	H (G)	δH (G)	Total Error (MHz)	$\nu_{\text{calc}} - \nu_{\text{exp}}$ (MHz)
<u>J = 5/2</u>						
11/2, -9/2 11/2, -3/2	11.713	.015	14.990	.015	.019	.006
	19.850	.030	24.970	.020	.034	-.011
	28.225	.020	34.980	.010	.022	.018
	32.525	.020	40.007	.015	.024	.039
	41.360	.020	50.018	.010	.022	.003
	50.424	.050	60.008	.020	.053	-.012
	41.415	.030	50.033	.020	.036	-.039
11/2, -11/2 11/2, 1/2	27.965	.020	34.980	.020	.026	.011
9/2, -7/2 9/2, -1/2	19.575	.015	24.980	.010	.017	-.005
	37.310	.025	45.019	.010	.027	-.005
<u>J = 3/2</u>						
9/2, -9/2 9/2, -3/2	5.715	.025	14.853	.010	.025	.022
	9.875	.025	24.984	.014	.026	.022
	14.215	.025	35.020	.010	.025	.006
	21.065	.010	50.003	.005	.010	-.003

$$\chi_{\text{min}}^2 = 6.2$$

$R_{5d} = -0.42$ for Pr and Tm. Murakawa found that $R_{5d} = -0.3$ for the states of the 5d configuration in ^{139}La [Murk-58].

Therefore, we adopt

$$Q^{139} = \frac{0.27(1-0.12)}{(1+0.40)} = + 0.17 \text{ b.}$$

The present experiments were not accurate enough to determine the sign of μ_I^{140} through its small contribution to H (see equation 3.15). However, Blok and Shirley [Blok-66] have found, using combined nuclear and solid state techniques, that $Q^{140} = +0.47 Q^{139}$, with 10% standard error*. Adopting their sign for Q^{140} we have:

$$\mu_I^{140} = (+) 0.73(3) \text{ n.m.}$$

$$Q^{140} = (+) 0.11(4) \text{ b.}$$

The errors include allowances for a possible 2% hfs anomaly and a 25% uncertainty in R_{5d} .

* Only their sign has been adopted because of the very uncertain nature of parameters used by Blok and Shirley. Since these authors only give the standard error, no real means exists for comparing their value with ours.

E. The ^{149}Nd Experiments

Samples of natural neodymium, in the form of single metal pellets enclosed in evacuated quartz vials, were irradiated in the McMaster reactor for four hours. The composition of the material was verified using neutron activation techniques and I am indebted to Dr. James Mason for providing the high resolution γ -spectrum. Three radioactive neodymium isotopes are produced by thermal neutron capture. The amount of 11-day ^{147}Nd present after a short irradiation is negligible. This is not the case for ^{151}Nd ($\tau_{1/2} = 12$ minutes), but one can delay the start of the beam experiments for approximately an hour to ensure that the activity has decayed before the buttons are counted. This leaves only the 1.8-hour ^{149}Nd isotope but, of course, the samples also contained the promethium daughter activities. Typical sample size was 200 mg which was sufficient to yield 50 mCi of ^{149}Nd .

The source material was loaded into a tantalum oven of similar design to that used in the lanthanum experiments. The oven power was set to about 180 watts which allowed the beam to last for about 3 hours. Fortunately, the beam intensity was very steady, exhibiting none of the wild fluctuations experienced in the lanthanum runs. Neodymium is readily detected with a hot-wire ionizer and so, at the beginning of each run, the oven was aligned to maximize the

signal-to-background ratio for the $J=4, I=0$ resonance in the even-even isotopes in the beam. This resonance was also used to check that no serious field shifts occurred during a run. Because of the characteristic beam stability, only two or three rf-off exposures were necessary. Buttons were exposed for 10-15 minutes which produced a counting rate of 300-600 c.p.m. for the monitor button.

Because of the presence of the promethium isotopes (50-hour ^{149}Pm and 28-hour ^{151}Pm) the automatic counting system was set to print out the counts accumulated from each resonance button at 40-minute intervals. Occasionally this sequence was interrupted and the higher-counting monitor buttons were placed in their respective counters for a short time. Counting was continued in this way for 12 hours after each run. The analysis of the decay data, using the computer programme FIX, has been described above.

The electronic configuration of the neodymium atom is $4f^4 6s^2$ which forms a ground multiplet 5I_J where $J = 4, 5, 6, 7$ and 8 . Experiments conducted using the even-even isotopes in a stable beam revealed that resonances in the $J=4$ state were approximately 50% more intense than those in $J=5$. According to the Boltzmann factor, the population of the $J=4, 5$ and 6 states should be in the ratio of 5:2:1 if an oven temperature of 1800°K is assumed [Budk-62]. However,

the g_J 's for $J=4$ and 5 are $-0.60324(10)$ and $-0.9002(2)$ respectively [Spal-63]. The expected relative intensities of the resonances follow from equation (4.4) noting that v_c^2 is proportional to g_J . Thus,

$$\frac{I(J=4)}{I(J=5)} \approx \frac{5}{2} \frac{-0.6}{-0.9} \approx 1.7,$$

which explains the observation.

The spin of ^{149}Nd has been determined to be $I=5/2$ [Budk-64]. Thus, for $J=4$, the possible F -values range from $3/2$ to $13/2$. For normal ordering, however, focussable Zeeman transitions occur only for $F=13/2$, $11/2$, $9/2$ and $7/2$. There should be five more observable transitions in $J=5$. Because J is integral for neodymium, the lowest multiplicity of any focussable Zeeman transition is two so that m_J can be changed from $+1$ to -1 or vice versa. The resonances in $F=13/2$ and $F=11/2$ ($J=4$) were used in this experiment to determine the $J=4$ hfs constants. Weaker resonances were also seen in $J=4$, $F=9/2$ and $J=5$, $F=5/2$ but, because of the overall consistency of the other data it was decided that it was unnecessary to obtain further resonances.

As was the case in the lanthanum experiment, the resonances in $F=13/2$ and $11/2$ are the superpositions up to second order in H , of several transitions. In particular, for $F=13/2$, there are 2-, 4-, 6- and 8-quantum transitions superimposed and, for $F=11/2$, 2-, 4- and 6-quantum transitions occur at the same frequency. Third order effects

were small enough to permit observations up to 90G without significant splitting. Figure 4.6 shows the 10 high-field resonances used to obtain A_4 and B_4 . The resonances in $F=13/2$ were fitted to the 6-quantum transition frequency and those in $F=11/2$ were treated as pure 4Q. Table 4.3 lists the data and the residuals obtained from LOLA. The results are:

$$|A_4| = 91.0(19) \text{ MHz}$$

$$|B_4| = 266(53) \text{ MHz}$$

and $B_4/A_4 > 0$

Again, the errors quoted represent one standard deviation of the χ^2 distribution. The values of A and B were not significantly changed when the data were reinterpreted by assigning the resonances to other transitions within the superimposed groups.

The nuclear moments for ^{149}Nd are found by again using the Fermi-Segrè relations. Either ^{143}Nd or ^{145}Nd can be used as the comparison isotope. The hfs constants for the $J=4$ states of both stable isotopes were measured by Spalding [Spal-63]. Smith and Unsworth have made direct measurements of the magnetic moments using atomic beam triple resonance [Smit-65]. In addition, these authors also deduced the quadrupole moments from the measured B's. The

Fig. 4.6 ^{149}Nd RESONANCES USED IN OBTAINING THE FINAL RESULTS

The crosses on the left hand side of some of these resonances are the rf-off intensity. As can be seen, good reproducibility was verified by repeating the resonances.

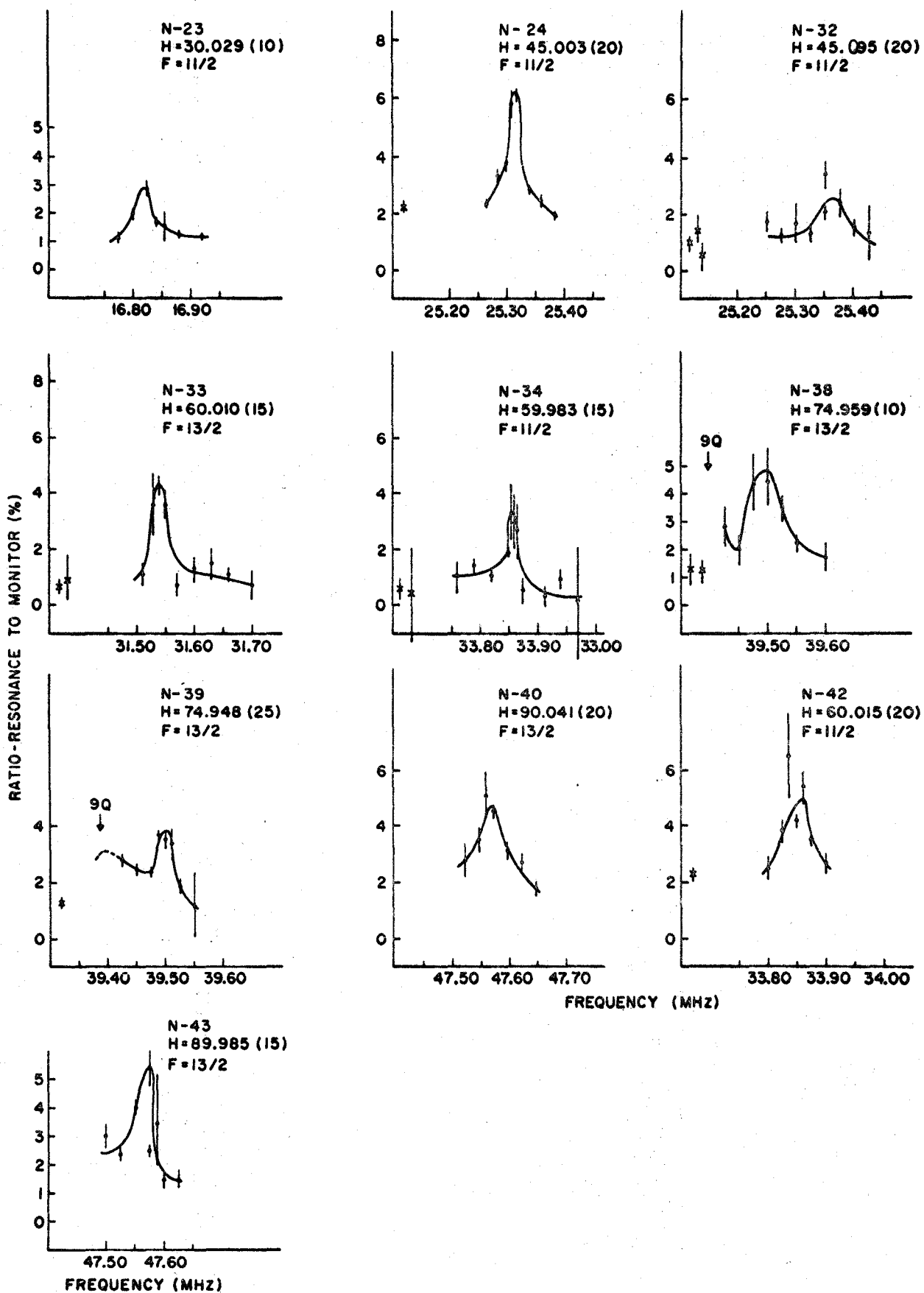


TABLE 4-3
The ^{149}Nd Resonances ($J=4$)

$ F, m_F\rangle \rightarrow F', m'_F\rangle$	ν_{exp} (MHz)	$\delta\nu_{\text{exp}}$ (MHz)	H (G)	δH (G)	Total Error (MHz)	$\nu_{\text{calc}} - \nu_{\text{exp}}$ (MHz)
$(13/2, 11/2) \rightarrow (13/2, -1/2)$	31.535	.010	60.010	.015	.013	-.001
	39.500	.015	74.959	.010	.016	+0.000
	39.500	.025	74.948	.035	.031	-.006
	47.570	.015	90.041	.020	.018	+0.013
	47.560	.010	89.985	.015	.013	-.007
$(11/2, 7/2) \rightarrow (11/2, -1/2)$	16.817	.010	30.029	.010	.012	-.003
	25.315	.010	45.042	.035	.022	-.028
	25.370	.015	45.095	.035	.025	-.007
	33.860	.010	59.983	.015	.013	+0.012
	33.860	.010	60.015	.010	.012	-.013

$$\chi_{\text{min}}^2 = 4.3$$

errors in Q include no allowance for uncertainty in the Sternheimer correction. The properties of the two isotopes are:

	^{143}Nd	^{145}Nd
I	7/2	7/2
A_4	-195.649 (9) MHz	-121.627 (27) MHz
B_4	+122.25 (29) MHz	+ 64.60 (37) MHz
μ_I	-1.063 (5) n.m.	-0.654 (4) n.m.
Q	-0.48 (2) b.	-0.25 (1) b.

Thus, from the present measurements, the moments of ^{149}Nd are:

$$\left| \mu_I^{149} \right| = 0.350 (10) \text{ n.m.}$$

$$|Q| = 1.3 (3) \text{ b.}$$

and

$$\mu_I/Q < 0.$$

The errors reflect the experimental uncertainties in the hfs constants for ^{149}Nd and also allow for a possible 1% hfs anomaly and allow for a 50% error in the shielding parameter R . The magnetic moment is corrected for diamagnetic shielding.

F. The ^{147}Nd Experiments

The study of 11-day ^{147}Nd followed as a natural extension of the ^{149}Nd experiments. The spin and magnetic moment of ^{147}Nd have been measured by Kedzie et al. [Kedz-57] using EPR and the spin was confirmed to be $I=5/2$ by an atomic beam experiment [Cabz-62]. Since both ^{149}Nd and ^{147}Nd have $I=5/2$, focussable transitions have the same quantum numbers for both isotopes. Our goal was to determine the quadrupole moment of ^{147}Nd so as to complete the data concerning the ground state quadrupole moments of all the accessible neodymiums.

Samples of natural neodymium metal, sealed in evacuated quartz vials, were irradiated in the McMaster reactor for a period of 14 days. In order to eliminate the promethium activities a minimum 6-day cooling period was allowed before the beam experiments were carried out. The sample activity was verified to be due to the decay of ^{147}Nd through the observation of the resulting γ -spectrum. I am indebted to Mr. Brian Cook for providing the γ -spectrum. In addition, a small amount of the sample was painted on a button and counted at intervals over a two-week period using one of the β -counters. The observed decay was consistent with a 11-day half life.

During the ^{147}Nd runs it was found that the rf-off

tended to be somewhat less constant over the course of a run than it had been for the ^{149}Nd experiments. It proved to be expedient to interpolate and subtract off the background from the resonance buttons in the same way as in the lanthanum experiments.

The 11-day half life of ^{147}Nd meant that the activity of the various buttons could be considered to be constant throughout the counting periods - typically 6 hours in duration - so that no corrections for decay were made. The resonances were observed in J=4 state only and they are shown in Fig. 4.7 .

For these experiments resonances were seen in the F=9/2 state as well as in F=13/2 and F=11/2. The resonances were assumed to be pure 6Q (F=13/2) and pure 4Q (F=11/2 and F=9/2) for utilization of the fitting programme LOLA. Again no significant changes in A and B resulted when other appropriate choices were used.

The hfs constants A_4 and B_4 are:

$$|A_4| = 143(4) \text{ MHz}$$

$$|B_4| = 181(64) \text{ MHz}$$

and $B_4/A_4 > 0$.

Table 4.4 gives the data and the residuals for the adopted values of the hfs constants. Again the errors in the hfs constants represent one standard deviation of the χ^2 distribution. Application of the Fermi-Segrè relations in

Fig. 4.7 ¹⁴⁷Nd RESONANCES

The rf-off background was interpolated and subtracted off as was the case for the lanthanum resonances. Unless otherwise noted, the $F=13/2$ resonances are predominantly 6Q and the $F=11/2$ and $F=9/2$ are 4Q. The term V_{opt} refers to the rf voltage applied to the loop to optimize the ³⁹K 1-Q resonance.

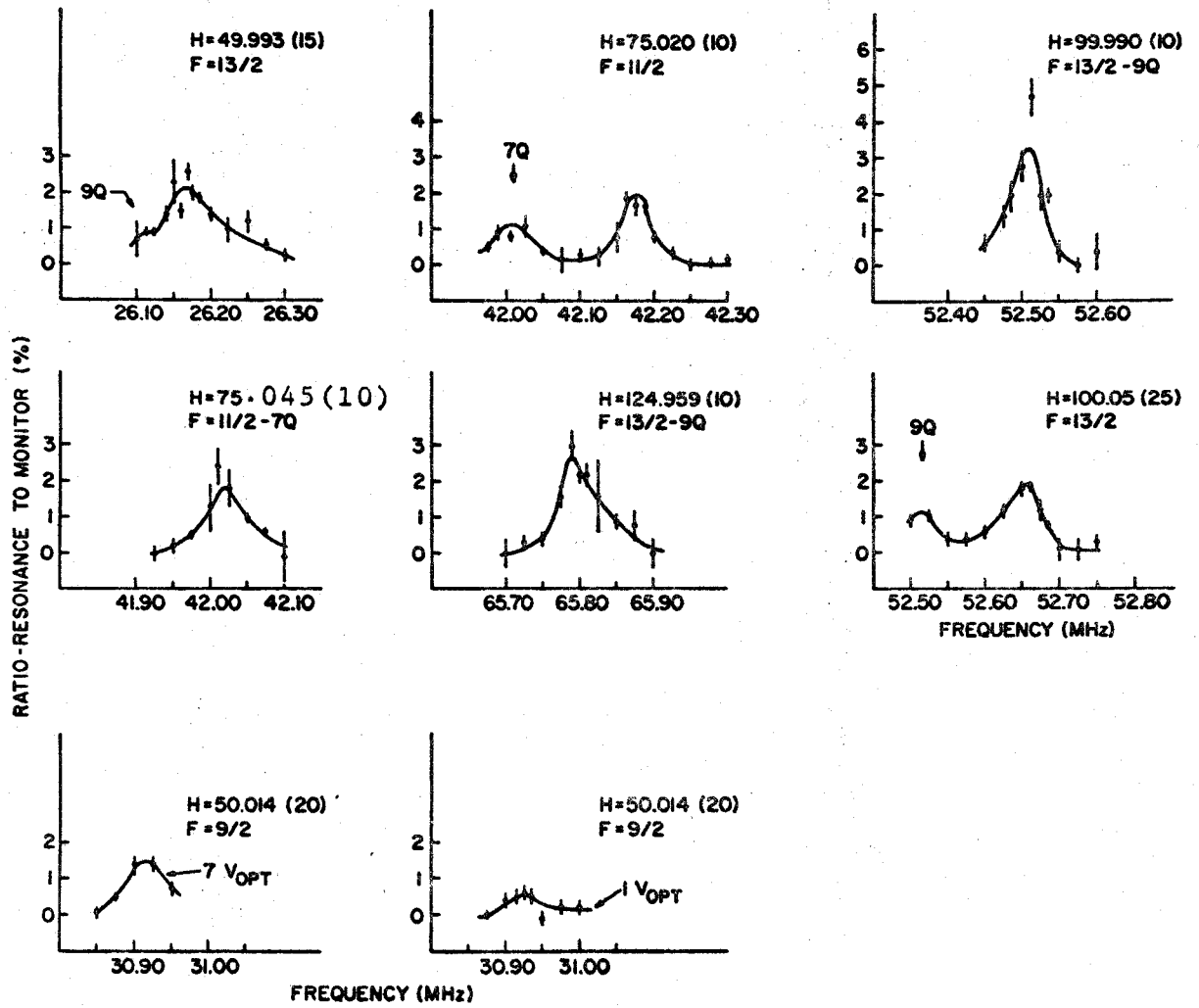


TABLE 4-4
The ^{147}Nd Resonances ($J=4$)

$ F, m_F\rangle \rightarrow F', m'_F\rangle$	ν_{exp} (MHz)	$\delta\nu_{\text{exp}}$ (MHz)	H (G)	δH (G)	Total Error (MHz)	$\nu_{\text{calc}} - \nu_{\text{exp}}$ (MHz)
(13/2, 11/2) (13/2, -1/2)	26.163	.025	49.993	.015	.026	-.012
	52.660	.015	100.005	.020	.018	+0.000
(13/2, 13/2) (13/2, 5/2)	52.515	.015	99.990	.010	.016	-.003
	65.790	.025	124.959	.010	.026	+0.010
(11/2, 7/2) (11/2, -1/2)	42.175	.015	75.020	.010	.016	+0.000
(11/2, 9/2) (11/2, -5/2)	42.010	.025	75.020	.010	.026	-.008
	42.018	.010	75.045	.010	.012	-.002
(9/2, 5/2) (9/2, -3/2)	30.920	.015	50.014	.020	.020	+0.002
	30.913	.025	50.014	.020	.030	+0.009

$$\chi_{\text{min}}^2 = 0.64$$

comparison with the moments and hfs constants of ^{145}Nd yields

$$|\mu_I| = 0.553(15) \text{ n.m.}$$

$$|Q| = 0.9(3) \text{ b.}$$

$$\mu_I/Q < 0,$$

where the quadrupole moment has been corrected for a net shielding of $R = +0.2(1)$. The magnetic moment includes the diamagnetic correction. The magnitude of μ_I is in fair agreement with the paramagnetic resonance value of Kedzie and the later data of Halford [Full-69] on the crystal field parameters.

CHAPTER V

DISCUSSION

A. The ^{140}La Results

The low-lying states of $^{140}_{57}\text{La}_{83}$ must come about from the coupling of the seven protons beyond the closed shell at $Z=50$ and the 83^{rd} neutron which is almost certainly in a $2f_{7/2}$ orbital. In this region, the proton orbitals $g_{7/2}$ and $2d_{5/2}$ appear to compete for ground state and first excited state. Thus, in $^{139}_{57}\text{La}_{82}$, a state of $I = 5/2$ is only 166 keV above the $I = 7/2$ ground state and these can be assumed to be predominantly $2d_{5/2}$ and $1g_{7/2}$ respectively. On the other hand, in $^{141}_{59}\text{Pr}_{82}$, the ground state has $I = 5/2$ and the spin of the first excited state is $7/2$.

In ^{139}La , the internal conversion coefficient shows that the 166-keV transition is predominantly M1 in character [Geig-65]. Furthermore, the γ -transition rate is hindered by a factor of 300 compared to the Weisskopf estimate. If one does suppose that the two proton states involved are $d_{5/2}$ and $g_{7/2}$, then a small amount of other configurations must be present because otherwise an M1 transition between them would not proceed at all.

An alternative explanation of ^{139}La is possible - namely, that the ground state proton configuration is

$(g_{7/2})_{7/2}^5 (d_{5/2})_0^2$ and the first excited state is $(g_{7/2})_{5/2}^5 (d_{5/2})_0^2$. Then the M1 transition would be totally forbidden because of the changes in seniority quantum number, so small amounts of other configurations would reproduce the experimental findings.

In the light of these ideas, we can expect the odd-odd nucleus ^{140}La to have a set of eight low-lying states due to the coupling of the $f_{7/2}$ neutron to the $j_p = 7/2$ proton configuration to produce $I = 0, 1, \dots, 7$. In addition, also at low energy, there should be a set of six states with $I = 1, 2, \dots, 6$ due to the coupling of the odd neutron to the $j_p = 5/2$ excited proton configuration. Because of the residual neutron-proton interaction states of the same I can mix. Thus the 3^- ground state, for example, would be the lower of the possible $I = 3$ states. The magnetic moment can be used to choose between the alternatives presented above.

Recalling equation (2.11), we have

$$\mu_{0-0} = \mu_N \left\{ \frac{I}{2} (g_p + g_n) + \frac{(g_p - g_n) [j_p(j_p + 1) - j_n(j_n + 1)]}{(2I + 1)} \right\}.$$

In accord with Cain's results (section II-C) the value for g_n should be taken from the known magnetic moments for $N=83$, even-odd nuclei. Since $\mu_I = 1.1$ n.m. for ^{141}Ce and $\mu_I = -1.06$ n.m. for ^{143}Nd [Full-69], $g_n = 0.31$. Similarly, g_p should be evaluated

from neighbouring odd-even nuclei. For a $g_{7/2}$ -proton the average of ^{135}Cs ($\mu_I = +2.73$ n.m.), ^{137}Cs ($\mu_I = +2.84$ n.m.) and ^{139}La ($\mu_I = +2.78$ n.m.) yields $g_p = +0.79$. The $d_{5/2}^-$ value comes from the moment of ^{141}Pr ($\mu_I = +4.3$ n.m.); for that proton configuration $g_p = +1.7$. The g_p for the seniority-3 coupling $(g_{7/2})_{5/2}^5$ should be the same as that for $g_{7/2}$ above (section II-C). On the basis of these values, then, the following moments are predicted for the ^{140}La ground state:

$$\begin{aligned} |\pi g_{7/2} \vee f_{7/2}; I=3 \rangle & \quad \mu_I = +0.72 \text{ n.m.} \\ |\pi d_{5/2} \vee f_{7/2}; I=3 \rangle & \quad \mu_I = +0.23 \text{ n.m.} \\ |\pi (g_{7/2})_{5/2}^5 \vee f_{7/2}; I=3 \rangle & \quad \mu_I = -0.24 \text{ n.m.} \end{aligned}$$

If the ground state is a mixture of the first two,

$$\alpha |\pi g_{7/2} \vee f_{7/2}; I=3 \rangle + (1-\alpha)^{1/2} |\pi d_{5/2} \vee f_{7/2}; I=3 \rangle,$$

then the moment is given by

$$\mu_I = 0.72 \alpha^2 + 0.23 (1-\alpha^2);$$

if it is a mixture of the first (amplitude= β) and the third,

$$\mu_I = 0.72 \beta^2 - 0.24 (1-\beta^2).$$

The measured moment of ^{140}La is $\mu_I = +0.73(3)$ n.m. indicating a virtually pure $g_{7/2}$ proton configuration. This is in sharp contrast to the case of the $I=3$ ground state of ^{138}Cs , which also has 83 neutrons. For it, $\mu_I = (+)0.48(10)$ n.m. [Stin-67] indicating a significant degree of configuration mixing.

Kern et al [Kern-67] used the (d,p) reaction on ^{139}La to investigate the low-lying levels of ^{140}La . It is known from direct reaction theory that the differential cross section $\frac{d\sigma}{d\Omega} \propto S (2I+1)$, where S is the so-called spectroscopic factor, which is proportional to the overlap between the wave functions of the initial and final states, and I is the spin of the final state. Under the assumption that only two active configurations contribute to the ^{140}La spectrum, the final states may be written

$$|I\rangle = \alpha |\pi g_{7/2} \nu f_{7/2}; I\rangle + (1-\alpha^2)^{1/2} |\pi d_{5/2} \nu f_{7/2}; I\rangle$$

and the orthogonal mixture,

$$|I\rangle' = (1-\alpha^2)^{1/2} |\pi g_{7/2} \nu f_{7/2}; I\rangle - \alpha |\pi d_{5/2} \nu f_{7/2}; I\rangle.$$

For $I = 0$ and 7 , $\alpha = 1$ and the second state doesn't exist because the $d_{5/2} f_{7/2}$ configuration can't form those angular momenta. Compared to the largest cross-section (for the formation of the spin-7 level), the relative cross-sections for the others become

$$\left(\frac{d\sigma}{d\Omega}\right)_{\text{rel}} = \frac{\alpha^2 (2I+1)}{15} \text{ and } \frac{(1-\alpha^2) (2I+1)}{15}.$$

Thus the spins of the observed levels, and the squares of their mixing amplitudes, can be determined. In particular, Kern et al. found for the ^{140}La ground state

$$|\text{g.s.}\rangle = 0.90 |\pi g_{7/2} \nu f_{7/2}; 3\rangle + 0.43 |\pi d_{5/2} \nu f_{7/2}; 3\rangle.$$

For such a mixture, the magnetic moment should be 0.62 n.m., which is only in fair agreement with our result.

More recently, Kemper et al. at Indiana State [Kemp-69] have measured the β - γ angular correlations in the decay of ^{140}La to ^{140}Ce . From the data and the calculated wave functions for the states involved in ^{140}Ce , they deduce that the mixing coefficient in the ground state of ^{140}La has the value $\alpha \approx 1.00(4)$. The error is an experimental one and no allowance is assigned to the calculation itself. Their result is, of course, in excellent agreement with our conclusion.

Two attempts have been made to explain the properties of the low-lying states of ^{140}La theoretically. Struble [Stru-67] used a variety of residual internucleon forces within a quasi-particle coupling model. The neutron was assumed to be in the $2f_{7/2}$ orbital, but the protons were allowed to have amplitudes in all the shell model states that come between the magic numbers at $Z=50$ and $Z=82$. With reasonable success he was able to fit the observed γ -transition rates, branching ratios and (d,p) cross-sections. Unfortunately, the calculated level ordering is not in accord with the observed spectrum (an $I=6$ state lies lowest) although the levels do "group" in the right places. The calculation is a noteworthy achievement, nevertheless, in that the requisite parameters (the strengths and radial dependence of the residual

interaction, and the shell model energies) have reasonable values.

Heyde and Brussaard [Heyd-68] have calculated the ^{140}La spectrum in terms of the unified model which seeks to combine collective oscillations of the nuclear core with shell model states (here $\pi g_{7/2}$, $\pi d_{5/2}$ and $\nu f_{7/2}$ for the odd nucleons). The procedure involved, in essence, the evaluation of the parameters of the model Hamiltonian by least-squares fitting the calculated eigenvalues to the observed energy levels. After several iterations, parameters which give the $d_{5/2}$ - $g_{7/2}$ gap, the strength of the phonon-proton and phonon-neutron coupling, the phonon energy and the strengths of the residual particle-particle interaction are generated and these values determine the spectrum. Although fair agreement exists between the calculated and experimental M1 transition rates, the calculated spectrum does not compellingly reproduce the observed spectrum, despite the fact that 10 of the 14 low energy levels were used in the least-squares fit. Indeed, the authors note that it was not possible to reproduce the known ground state spin. They suggest, however, that an $I=3$ might be depressed far enough by more appreciable mixing in a larger configuration space. Such a solution would not be consistent with our finding that the ground state may be considered essentially pure.

B. The ^{149}Nd Results

According to the simple shell model, $^{149}\text{Nd}_{89}$ should have 7 neutrons in the $2f_{7/2}$ orbital, which is to say, one $2f_{7/2}$ hole. However, the measured spin of the ground state is $5/2$ [Budk-64]. One might suppose, therefore, that residual interactions make it favorable to have configurations such as $\nu(2f_{7/2})_{5/2}^5 (h_{11/2})_0^2$, $\nu(2f_{7/2})_{5/2}^5 (3p_{3/2})_0^2$ or $\nu(2f_{7/2})_0^6 (2f_{5/2})_{5/2}$. For the spherical shell model to be applicable, however, the ground state quadrupole moment should be quite small, say $< 0.2 b$ (section II-b). In view of the fact that our value for Q is $\pm 1.3(3)b$, we are led to interpret ^{149}Nd in the light of the Nilsson model.

Indeed, there is a fair amount of evidence for this interpretation besides the magnitude of Q . An isotone of ^{149}Nd , $^{153}\text{Gd}_{89}$ has recently been shown to have levels whose life-times are consistent with the $M1/E2$ ratio to be expected in the rotational bands of distorted nuclei [Andr-69]. Furthermore, Nielson and Wilsky [Niel-68], who investigated the level structure of ^{153}Gd using conversion electrons and gamma coincidence techniques, note that the very high level density in the vicinity of the ground state is indicative of permanent nuclear deformation.

A useful indication of changes in nuclear shape is provided by mass spectroscopic studies of the double neutron separation energy (S_n) and the neutron pairing energy (P_n).

Duckworth and legions have shown [Duck-69], for neodymium and samarium, that there is a pronounced dip in S_n and a peak in P_n in the vicinity of $N=89$ as one progresses from $N = 82$ to $N = 90$. Such features are interpreted to mean that the shape of the nucleus changes from spherical to ellipsoidal. In accord with the result of Duckworth et al, several authors have attempted to interpret the levels of ^{151}Sm in terms of the Nilsson model.

Nealy [Neal-65] used the direct reactions $^{148}\text{Nd}(d,p)^{149}\text{Nd}$ and $^{150}\text{Nd}(d,t)^{149}\text{Nd}$ to observe the energy levels populated in ^{149}Nd . Since the ^{148}Nd is spherical with a classic $0+, 2+, 2+$ vibrational spectrum and ^{150}Nd exhibits a rotational spectrum, Nealy argued that either the (d,p) or the (d,t) cross-section should be enhanced depending on whether a given level in ^{149}Nd is spherical or distorted. While his data do indicate a large number of states at low excitation, they don't lend themselves to any clear-cut decisions on the shape of the nucleus.

In the region of small deformation, the contribution of the Coriolis force on $K = \frac{1}{2}$ orbitals and the $\Delta N=2$ - mixing due to the quadrupole interaction can alter the customary $I(I+1)$ appearance of rotational bands. Expanding the Hamiltonian to calculate the mixing of states by these processes, Borggreen, Løvholden and Waddington [Borg-69] very successfully predicted, among other data, the energies

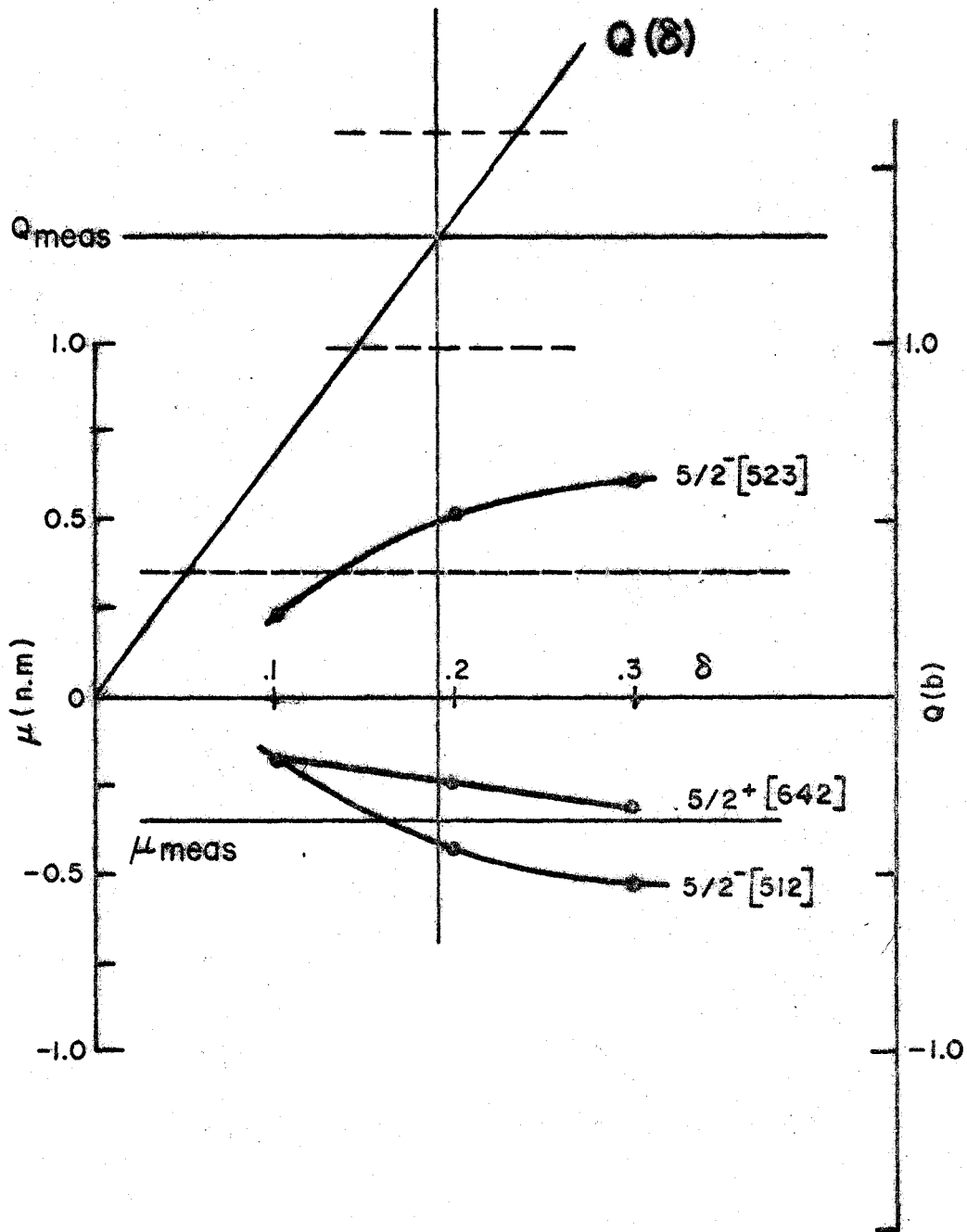
and cross-sections of levels in ^{155}Gd populated in the $^{156}\text{Gd}(d,t)^{155}\text{Gd}$ reaction. Contrary to the unperturbed "zeroth-order" Nilsson scheme, their results showed that positive parity states, of presumed high excitation energy, were greatly depressed. The fact that the levels Nealy saw in ^{149}Nd don't correspond to the $I(I+1)$ rule is taken as an indication that configurations of the type evident in ^{155}Gd may be important in ^{149}Nd also.

Provided that $K \neq \frac{1}{2}$, then systematics for the lanthanide region indicate that the deformation parameter δ is positive and hence we adopt $Q = (+)1.3(3)$ b for ^{149}Nd which implies that $\mu_I = (-)0.350(10)$ n.m. because $B/A > 0$. Using equation (2.17) to find the intrinsic quadrupole moment Q' and solving for δ from equation (2.20), we obtain $\delta = 0.18(4)$. In the region of $N = 89$ the only Nilsson levels available which have $\Omega = 5/2$ for this small positive deformation are $5/2+[642]$, $5/2-[523]$ and $5/2-[512]$. Although the work of Borggreen et al. indicates that it may be very dangerous to attempt to interpret a nucleus having a small deformation ($\delta < 0.3$) in terms of pure Nilsson states we are forced to do just that because of the lack of detailed reaction data concerning the ^{149}Nd levels.

Figure 5-1 is a plot of the magnetic moments of the three $\Omega = 5/2$ states as a function of deformation. Because no satisfactory evidence is available about the

Fig. 5.1 NUCLEAR MOMENTS OF $I = 5/2$ NILSSON STATES
AND ^{149}Nd MOMENTS

The effective g-factor, $g_n = 0.6 (g_n)_{\text{free}}$ was used. The quadrupole moment has been corrected for a net shielding of 12%. The vertical line is the deformation δ as determined by the observed value of $Q = (+)$ 1.3(3) b. Because experimentally $\mu_I/Q < 0$, the $5/2-[523]$ state is rejected since it predicts $\mu_I > 0$ for positive δ . As can be seen, no real distinction can be made on the basis of the data between the $5/2+[64]$ and $5/2-[512]$ states.



amount of inter-configuration mixing we have applied the commonly used ad hoc rule that $g_n \text{ eff} = 0.6 g_n \text{ free}$ [Kerm-56] and further we use $g_R = 0.2$ as is the case for ^{150}Nd [Pres-62]. It is seen that the $5/2-[523]$ orbital predicts a positive moment while both the $5/2+[642]$ and $5/2-[512]$ orbitals have negative moments. Therefore the first possibility is ruled out if $\mu_I < 0$. Reference to Fig. 5.1 reveals that no definite choice can be made between the $5/2+[642]$ and $5/2-[512]$ orbitals in the vicinity of $\delta \approx 0.18$

The log ft value for the β -decay of 2.3-minute $^{149}_{59}\text{Pr}_{90}$ to the ground state of ^{149}Nd is 5.9 [Vank-67]. This means that probably the transition is allowed or first forbidden [Gall-62]. Presuming that ^{149}Pr is also distorted with a $\delta \approx 0.2$, then the 59^{th} proton has available to it the states $1/2-[550]$, $3/2-[541]$, $3/2-[411]$, and $5/2+[413]$. For β -transitions the asymptotic quantum numbers $[N n_3 \Lambda]$ have selection rules which must be obeyed if the transitions are not to be hindered [Alag-57]. None of the states for the 59^{th} proton are consistent with an allowed transition, $(\Delta N, \Delta n_z, \Delta \Lambda) = (0, \pm 1, 0)$, to the ground state of ^{149}Nd - presumed to be either $5/2+[642]$ or $5/2-[512]$. The possibilities consistent with a first-forbidden transition are summarized in Table 5.1. The possible transitions are indicated by the arrows. Unfortunately, no definite choice for the ^{149}Nd ground state can be made on the basis of these considerations.

TABLE 5-1

Possible β -Transitions for $^{149}\text{Pr} \rightarrow ^{149}\text{Nd}$ on Nilsson Model

Proton	Neutron	ΔI	$\Delta \pi$	$(\Delta N \ \Delta n_3 \ \Delta \Lambda)$
1/2-[550]	5/2+[642]	2	yes	(-1 +1 -2)
	5/2-[512]	2	no	(0 4 -2)
3/2-[541] \longrightarrow	5/2+[642]	1	yes	(-1 0 -1)
	5/2-[512]	1	no	(0 3 -1)
3/2+[411] \searrow	5/2+[642]	1	no	(-2 3 -1)
	5/2-[512]	1	yes	(-1 0 -1)
5/2+[413] \searrow	5/2+[642]	0	no	(2 -3 1)
	5/2-[512]	0	yes	(-1 0 +1)

C. The ^{147}Nd Results

As was pointed out above, the ^{147}Nd experiments were undertaken so as to complete the measurements of Q for all the odd-A neodymium isotopes. The systematics of this region strongly indicate that $Q > 0$ - combining this with the measured ratio $B_4/A_4 > 0$ we obtain:

$$\mu_I = -0.553(15) \text{ n.m.}$$

$$Q = +0.9(3) \text{ b.}$$

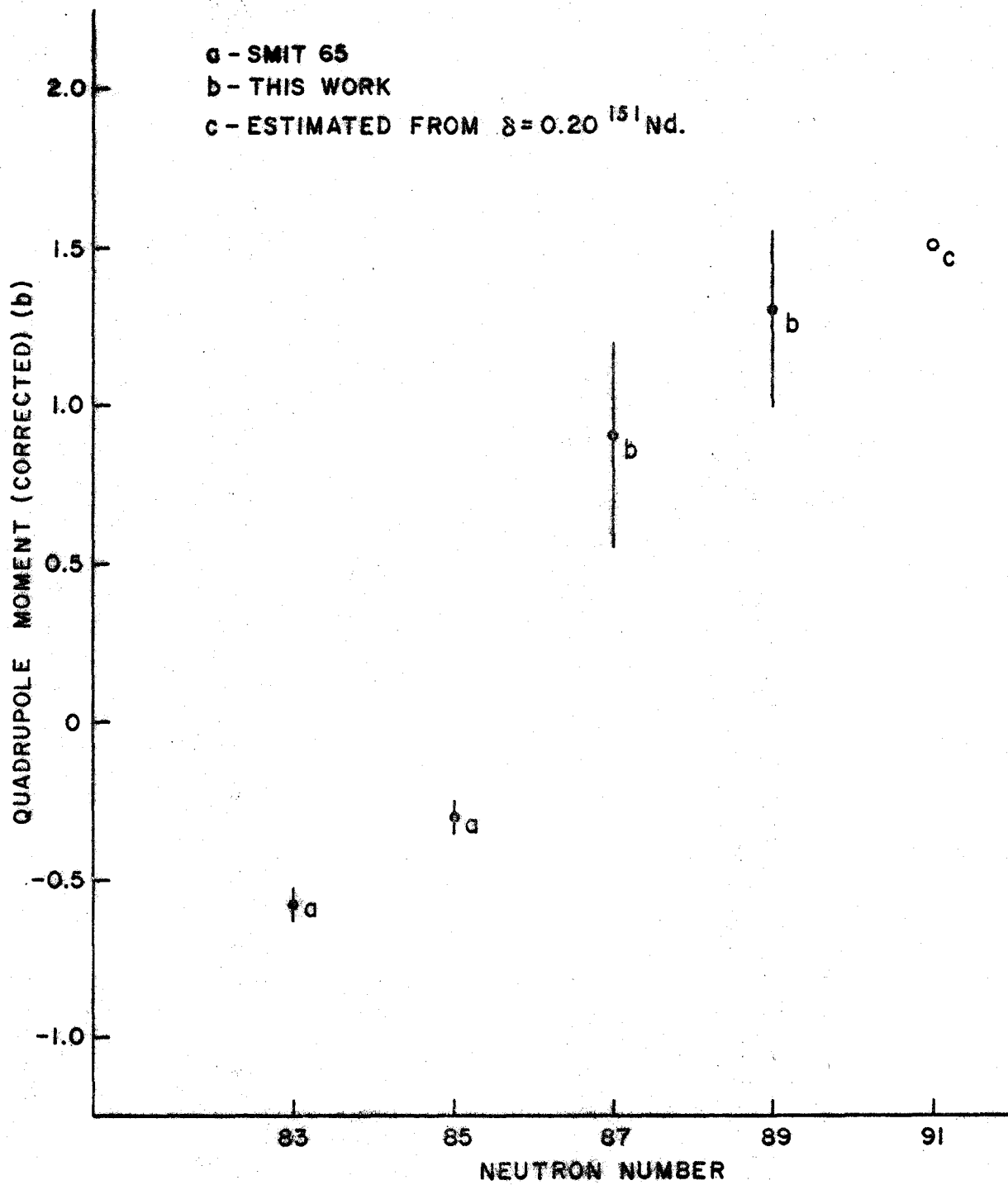
The size of the quadrupole moment is large but in terms of δ it yields $\delta_{(147)} = 0.12(4)$, which is quite small for simple Nilsson model arguments. It is interesting to note that ^{147}Pm also has a moderately large Q for its $I = 7/2$ ground state ($|Q| = 0.8(3)^*$ [Budk-63]) indicating the "softness" of the core for these nuclei. Nealy (op cit) has shown from (d,p) reaction study on ^{150}Nd that ^{151}Nd exhibits a rotational spectrum. Reasonable agreement with experiment resulted for the choice $\delta = 0.2$. Figure 5.2 is a plot, based on the above data, of the ground state quadrupole moments of the odd-A neodymium isotopes. The onset of nuclear deformation is clearly demonstrated.

The spin $5/2$ ground state of ^{147}Nd could be accounted for by a coupling of the type $(f_{7/2})_{5/2}^{-3}$, since

*The correction factor $R = .2$ has been applied to Budick's results

Fig. 5.2 GROUND STATE QUADRUPOLE MOMENTS OF ODD-A
NEODYMIUMS

All these moments have been adjusted for
a net 12% shielding-type Sternheimer
correction.



such states are frequently near to, or even form, the ground state [Kiss-66]. Because the g-factor for k nucleons in a state is the same as for one nucleon in that state (see II-C), the moment is reduced to $\frac{j-1}{j}$ of its original value. Typically the moments of these states have signs which would put them into the wrong Schmidt groups [Barr-69] and so the presence of these states is announced in this way. For ^{147}Nd the predicted moment would be $5/7(-1.1) = -0.78$ n.m. which is in fair agreement with the measured value. However, Kisslinger and Sorenson [Kiss-63] predict that for the 3 quasi-particle coupling $(f_{7/2}^{-3})_{5/2} Q = -0.38$ b, in strong disagreement with our result $Q = +0.9(3)$ b.

Although there is a strong branch to the $I = 5/2$ first excited state of ^{147}Pm in the β^- decay of ^{147}Nd , there is only a very weak branch to the $I = 7/2$ ground state [Beek-66]. The size of the quadrupole moment for ^{147}Nd indicates that this nucleus is just on the edge of deformation. Thus one might expect that the ground state would show the interconfiguration mixing of several shell model states. Such interconfiguration mixing has the effect that it can greatly reduce β^- transition probabilities.

D. Summary

In summary, then, the magnetic dipole and electric quadrupole moments of ^{140}La , ^{149}Nd and ^{147}Nd have been determined by atomic beam resonance methods. The corrections and uncertainties involved in translating the measured hfs constants to nuclear moments were discussed. Finally, the relationship between these nuclear moments and other known properties of the nuclei was developed.

Several additional experiments, related to this work come to mind. The effective magnetic moment of the 83rd neutron, used in determining the lanthanum ground state configuration, was based on the measured moment of ^{143}Nd and ^{141}Ce . It should be feasible to check that value by determining the magnetic moment of 81-minute $^{139}_{56}\text{Ba}_{83}$ through the use of ABMR. Since the electronic ground state of ^{139}Ba is $6s^2\ ^1S_0$, the atoms would have to be excited into another electronic state, for example $6s5d\ ^3D_J$, so that the atoms could be deflected by the A and B magnets. Excitations into the 6s5d configuration should be possible through a thermally heated "snout" on the oven or by microwave stimulation.

It was demonstrated in this work that ^{149}Nd is permanently distorted; it is the lightest lanthanide to show such distortion. Of course a complete reaction study would be very helpful in better understanding the ground

state nuclear magnetic moment. In particular, the determination of the ground state parity would be useful. Furthermore, it is interesting that ^{149}Pr exhibits such a propensity to beta decay to the ground state of ^{149}Nd . Reaction studies, such as $^{150}\text{Nd}(d, ^3\text{He})^{149}\text{Pr}$, to populate levels in ^{149}Pr would prove enlightening.

For comparison with Nealy and Sheline's published work on ^{151}Nd [Neal-67] a spin determination of 12-minute ^{151}Nd should be undertaken by ABMR.

Finally, the relative signs of μ_I and Q for ^{147}Nd seem to be in strong disagreement with the calculations of Kisslinger and Sorenson. The ABMR experiments should be extended to determine the absolute sign of μ_I so that the sign of the quadrupole moment can be definitely established.

BIBLIOGRAPHY

- Alag-57 Selection Rules for Beta and Gamma Particle
Transitions in Strongly Deformed Nuclei.
Alaga G
Nucl Phys 4. 625 (1957).
- Andr-69 Nanosecond Isomeric Transitions in the 89-
Neutron Nucleus ^{153}Gd .
Andrejtscheff W, Meiling W and Stary F
Nucl Phys A137. 474 (1969)
- Arma-55 Configuration Mixing and Magnetic Moments of
Odd Nuclei.
Arima A and Horie H
Prog Theor Phys (Japan) 12. 623 (1954)
- Barr-69 Interpretation of some Neutron States for A=140-150.
Barrett PH and Shirley DA
Phys Rev 184 (4). 1185 (1969).
- Beek-66 Beta Decay of ^{147}Nd
Beekhuis H, Boskma P, van Klinken J and de Waard H
Nucl Phys 79. 220 (1966)
- Blin-54 The Deviation of Nuclear Magnetic Moments From
the Schmidt Lines.
Blin-Stoyle RJ and Perks MA
Proc Phys Soc A67. 885 (1954)
- Bloc-40 Magnetic Resonance for Nonrotating Fields .
Bloch F and Siegert A
Phys Rev 57. 522 (1940)
- Blok-66 Nuclear Orientation of ^{140}La , ^{154}Eu , ^{159}Gd ,
 ^{177}Lu , and $^{197\text{m}}\text{Lu}$ by Sternheimer Antishielding.
Blok J and Shirley DA
Phys Rev 143. 911 (1966)
- Bohr-50 Influence of Nuclear Structure of Hyperfine
Structure of Heavy Elements.
Bohr A and Weisskopf VF
Phys Rev 77. 94 (1950)

- Bohr-51 Nuclear Magnetic Moments and Atomic Hyperfine Structure (Collective Effects).
Bohr A
Phys Rev 81. 331 (1951).
- Bohr-53 Collective and Individual-Particle Aspects of Nuclear Structure.
Bohr A and Mottelson BR
Dan Mat Fys Medd 27(16). (1953)
- Bohr-58 Possible Analogy Between the Excitation Spectra of Nuclei and Those of the Superconducting Metallic State.
Bohr A, Mottelson BR and Pines D
Phys Rev 110. 936 (1958)
- Borg-69 Mixing of the Positive Parity States in ^{155}Gd .
Borggreen J, Løvholden G and Waddington JC
Nucl Phys A131. 241 (1969).
- Bren-60 jj Coupling Model in Odd-Odd Nuclei.
Brennan MH and Bernstein AM
Phys Rev 120. 927 (1960)
- Budk-62 Investigation of Electronic and Nuclear Properties of Some Rare Earth Isotopes (Spins of ^{161}Ho , ^{165}Er , ^{143}Pr and ^{149}Nd ; g_J For Ho; $|A|$ and $|B|$ for ^{147}Pm and ^{151}Pm and Inferred g_J and μ_I for the Pm isotopes).
Budick B
Ph.D. Thesis Univ of Calif, Report UCR2-10245, 1962
- Budk-63 Hyperfine Structure and Nuclear Moments of Promethium-147 and Promethium-151.
Budick B and Marrus R
Phys Rev 132. 723 (1963)
- Budk-64 Atomic-Beam Studies of Nuclear Properties of Some Rare-Earth Isotopes (Nuclear Spins of ^{143}Pr , ^{149}Nd , ^{161}Tb , ^{161}Ho , and ^{165}Er ; hfs Constants $|A|$ and $|B|$ of ^{171}Er and hfs Constant $|A|$ of ^{171}Tm).
Budick B, Maleh I and Marrus R
Phys Rev 135. B1281 (1964)

- Cabz-60 Nuclear Spins of Neodymium-147 and Promethium-147.
Cabezas A, Lindgren I, Lipworth E, Marrus R and
Rubenstein M
Nucl Phys 20, 509 (1960)
- Cain-58 Configurational Mixing in β -Decay Theory.
Caine CA
Proc Phys Soc (London) A71. 939 (1958)
- Cain-56 The Magnetic Moments of Odd-Odd Nuclei.
Caine CA
Proc Phys Soc (London) A69, 635 (1956)
- Came-62 The Magnetic Moment of Indium-115m.
Cameron JA, King HJ, Eastwood HK and Summers-Gill RG
Can J Phys 40, 931 (1962)
- Chil-69 Childs WJ
Private Communication (1969)
- Desh-63 de-Shalit A and Talmi I
Nuclear Shell Theory. Academic Press, New York (1963)
- Duck-69 Neutron Separation and Pairing Energies in the Region
 $82 \leq N \leq 126$.
Duckworth HE, Barber RC, Van Rookhuysen P, Macdougall
JD, McLatchie W, Whinery S, Bishop RL, Meredith JO,
Williams P, Southon G, Wong W, Hogg BG and Kettner ME
Phys Rev Lett 23 (11). 592 (1969).
- Eder-65 Eder G
Nuclear Forces; Introduction to Theoretical Nuclear
Physics (Trans. by I. Kaplan), MIT Press 1968.
- Full-69 Fuller GH and Cohen VW
Nuclear Data Tables, Academic Press, New York, 5 (5-6)
March 1969
- Gall-62 Two-Quasi-Particle States in Even-Mass Nuclei
with Deformed Equilibrium Shape.
Gallagher CJ and Soloviev VG
Mat Fys Skr Dansk Vid Selsk 2(2). 1962

- Geig-65 Measurements of M1 and E1 Transition Probabilities
in ^{125}Te , ^{127}Xe , ^{133}Cs , ^{139}La and ^{141}Pr .
Geiger JS, Graham RL, Bergstrom I and Brown I
Nucl Phys 68. 352 (1968)
- Good-68 Hyperfine Structure of Low Atomic Levels of ^{139}La .
Goodman LS and Childs WJ
Bull Am Phys Soc 13. 20 (1967).
- Habs-63 The Nuclear Moments of ^{13}N and ^{11}C .
Haberstroh RA
Ph.D. thesis Princeton Univ. 202 p. Technical
Report PUC-1963-69 (1963)
- Hack-56 Multiple Quantum Transitions of a System of Coupled
Angular Momenta.
Hack NM
Phys Rev 104. 84 (1956)
- Happ-64 Frequency Shifts in Atomic Beam Resonances
Happer W
Ph.D. Thesis, Princeton Univ. Report PUC-1964-148 (1964)
- Haxl-49 On the "Magic Numbers" in Nuclear Structure.
Haxel O, Jensen JHD and Suess HE
Phys Rev 75. 1766 (1949)
- Hofs-63 Hofstadter R
Electron Scattering and Nuclear Structure; a
Collection of Reprints with an Introduction.
Benjamin, New York, 1963
- Heyd-68 The ^{140}La Spectrum According to the Unified Model.
Heyde K and Brussaard PJ
Nucl Phys A112. 494 (1968)
- Hufn-65 Hyperfine Fields in Erbium Metal (and Application
of Sternheimer Correction).
Hüfner S, Kienle P, Wiedemann W and Eicher H
Z Phys 182. 499 (1965)

- Jaco-67 The Decay of ^{147}Nd .
Jacobs E, Heyde K, Dorikens M, Demoyneck J and
Dorikens-VanPraet L
Nucl Phys A99. 411 (1967)
- Kedz-57 Paramagnetic Resonance Hyperfine Structure of
 ^{141}Ce and ^{147}Nd .
Kedzie RW, Abraham M and Jeffries CD
Phys Rev 108. 54 (1957)
- Kerm-56 Rotational Perturbations in Nuclei - Application
to Wolfram 183.
Kerman AK
Dan Mat Fys Medd 30 (15). (1956)
- Kern-67 Study of the Levels in ^{140}La by (d,p) Stripping
Reaction.
Kern J, Struble GL and Sheline RK
Phys Rev 153. 1331 (1967)
- Kemp-69 Beta-Gamma Directional Correlation of the Outer
Group Decay in ^{140}La .
Kemper KW, Murphy RD and Wilkinson RG
Nucl Phys A124. 289 (1969)
- King-60 Atomic Beam Resonance Determination of the
Spins of Radioactive Nuclei.
King H
Ph.D. Thesis, McMaster Univ. 1960 (unpublished)
- Kiss-63 Spherical Nuclei with Simple Residual Forces.
Kisslinger LS and Sorenson RA
Rev Mod Phys 35. 853 (1963)
- Kiss-66 A Note on Coupling Schemes in Odd-Mass Nuclei.
Kisslinger LS
Nucl Phys 78. 341 (1966)
- Kopf-58 Kopfermann, H.
Nuclear Moments. Academic Press, New York 1958.
- Mayr-49 On Closed Shells in Nuclei.
Mayer MG
Phys Rev 75. 1969 (1949)

- Mayr-55 Mayer MG and Jensen JHD
Elementary Theory of Nuclear Shell Structure.
Wiley, New York, 1955
- Murk-58 Quadrupole Moments of ^{75}As , ^{139}La , and ^{201}Hg .
Murakawa K
Phys Rev 110. 393 (1958)
- Murk-61 Quadrupole Coupling in the Hyperfine Structure of
the Spectrum of LaI.
Murakawa K
J Phys Soc Jap 16. 2533 (1961)
- Neal-65 Nuclear Structure of ^{143}Nd , ^{149}Nd , and ^{151}Nd .
Nealy CL
Ph.D. Thesis Florida State Univ 1965 (unpublished)
Available from Univ. Microfilms Ann Arbor Mich.
- Neal-67 Nuclear Level Structure of ^{151}Nd .
Nealy CL
Phys Rev 164. 1503 (1967)
- Nier-57 The Measurement of the Nuclear Spins and Static
Moments of Radioactive Isotopes.
Nierenberg WA
Annual Rev Nucl Sci 7. 349 (1957).
- Niel-68 Levels in the 89-Neutron Nucleus ^{153}Gd .
Nielsen HL and Wilsky K
Nucl Phys A115. 377 (1968).
- Nils-55 Binding States of Individual Nucleons in Strongly
Deformed Nuclei.
Nilsson SG
Dan Mat Fys Medd 29 (16). 1955
- Nord-51 Nuclear Shell Structure and Beta-Decay. 2. Even
A Nuclei.
Nordheim LW
Rev Mod Phys 23. 322 (1951).
- Noya-58 Nuclear Moments and Configuration Mixing.
Noya H, Arima A and Horie H
Prog Theo Phys Jap (supp) 8. 33 (1958)

- Perl-69 Hyperfine Anomaly in ^{193}Ir by Mössbauer Effect,
and its Application to the Determination of Orbital
Point of Hyperfine Fields.
Perlow GJ, Henning W, Olson D and Goodman GL
Phys Rev Lett 23 (13). 680 (1969)
- Pete-60 Nuclear Spin of Lanthanum-140.
Peterson FR and Shugart HA
Bull Am Phys Soc 5 (5). 343 (session D-7) (1960)
- Pier-66 Multiple Quantum Transitions in Atomic Beam
Magnetic Resonance.
Pierce AR
M.Sc. Thesis McMaster Univ 1966 (unpublished)
- Pres-62 Preston MA
Physics of the Nucleus. Addison Wesley, Reading
Mass, 1962
- Rabi-37 Space Quantization in a Gyating Magnetic Field .
Rabi II
Phys Rev. 51. 652 (1937)
- Rain-50 Nuclear Energy Level Argument for a Spheroidal
Nuclear Model.
Rainwater J
Phys Rev 79. 432 (1950).
- Rams-56 Ramsey NF
Molecular Beams. Oxford, Clarendon Press, 1956
- Rein-58 Finite Size Effects on M1 Conversion Coefficients.
Reiner AS
Nucl Phys 5. 544 (1958)
- Salw-55 Resonance Transitions in Molecular Beam Experiments.
1. General Theory of Transitions in Rotating
Magnetic Field.
Salwyn H
Phys Rev 99. 1274 (1955)

- Schw-55 Theory of Hyperfine Structure.
Schwartz C
Phys Rev 97. 380 (1955)
- Smit-65 The Hyperfine Structure of ^{167}Er and Magnetic
Moments of $^{143,145}\text{Nd}$ and ^{167}Er by Atomic Beam
Triple Magnetic Resonance.
Smith KF and Unsworth PJ
Proc Phys Soc (London) 86. 1249 (1965)
- Spal-63 The Hyperfine Structure and Nuclear Moments of
 ^{143}Nd and ^{145}Nd .
Spalding IJ
Proc Phys Soc (London) 81. 156 (1963)
- Ster-50 Nuclear Quadrupole Moments.
Sternheimer RM
Phys Rev 80. 102 (1950)
- Ster-67 Quadrupole Shielding and Antishielding Factors
for Atomic States.
Sternheimer RM
Phys Rev 164. 10 (1967)
- Stin-67 The Spin and Magnetic Moment of ^{138}Cs .
Stinson GL, Archer NP, Waddington JC and Summers-
Gill RG
Can J Phys 45. 3393 (1967)
- Strk-62 Configuration Mixing and Effects of Distributed
Nuclear Magnetization on Hyperfine Structure in
Odd-A Nuclei.
Stroke, HH, Blin-Stoyle RJ and Jaccanino V
Phys Rev 123. 1326 (1961)
- Stru-67 Quasiparticle Model for ^{140}La .
Struble GL
Phys Rev 153. 1347 (1967)

- Ting-57 Hyperfine Structure and Quadrupole Moment of
Lanthanum-139.
Ting Y
Phys Rev 108. 295 (1957)
- Vand-67 Hyperfine Structure Separation, Nuclear Magnetic
Moments, and Hyperfine Structure (hfs Anomalies
of Gold-198 and Gold-199).
Vanden Bout PA, Ehlers VJ, Nierenberg WA and Shugart HA
Phys Rev. 158. 1078 (1967)
- Vank-67 Existence and Decay of ^{149}Pr
Van Klinken J and Taff LM
Nucl Phys A99. 473 (1967)
- Wybn-65 Wybourne BG
Spectroscopic Properties of Rare Earths. Interscience
New York, 1965